2084 *Bull. Chem. Soc. Jpn. Vol. 80, No. 11, 2084–2109 (2007)*

*Award Accounts*

**The Chemical Society of Japan Award for Creative Work for 2005**

# Smart Photoresponsive Polymer Systems Organized in Two Dimensions

**Takahiro Seki**

Department of Molecular Design and Engineering, Graduate School of Engineering, Nagoya University,
Chikusa-ku, Nagoya 464-8603

Received April 25, 2007; E-mail: tseki@apchem.nagoya-u.ac.jp

Light can be used as a precise stimulus by selecting suitable wavelengths, polarization directions, and intensity, allowing non-contact control. When photoresponsive (mostly photochromic) molecular units are combined with polymeric materials and liquid-crystalline materials, various types of smart photofunctions can be created. Smart functions involve photomechanical responses, photoalignment of anisotropic materials, orientational amplifications, photoinduced phase changes, photo-tuning of microphase separated structures in block copolymers, and so forth. This article reviews our research strategies, backgrounds, and topics to put forth smart functions in polymer systems organized in two dimensions. It is anticipated that light-driven smart film systems will find many versatile applications as promising future materials.

## 1. Introduction

Among many choices of external stimuli to trigger material motions, light is particularly fascinating. Light approaches materials in non-contacting manners with high addressing accuracy. Furthermore, light can be modulated in terms of intensity, energy (wavelength), polarization, coherency, spatial multiplicity, etc. In principle, molecular assemblies possessing ordered arrangement can effectively receive such types of light information. When photochromic molecules are utilized, reversible or repeatable functionalities are further available.

In this review article, several topics concerning our attempts to create smart photoresponsive functions based on 2-dimensional (2D) organizations are summarized. The term "smart" implies that the systems involved here are not based on simple on–off switching, but exhibit a great deal of secondary effects, such as cooperative assembling alternations, orientational amplifications, etc., which are triggered and initiated by an excited ("hot") molecule. Our approach basically adopts 2D material systems, such as monolayers on water and ultrathin films, because factors making complex situations in 3D systems are eliminated, and the material responses may be directly correlated with the events of molecules. Materials with lower dimensionality are prototypes, which effectively tell us the extent of ultimate response abilities ideally derived from the molecular functions.

In Fig. 1, the reversible photoisomerization reaction of azobenzene (Az)[1,2] and (2 + 2) cycloaddition between two cinnamoyl units[3,4] are shown as representative useful examples of a photoreaction. Most systems dealt with in this article are based on the Az units, and some parts utilize cinnamoyl groups. Motional correlations between "hot" molecules and materials are by no means simple but should be understood by considering the hierarchies. The molecular functions possessed by the photoreactive moiety, in general, are not actually reflected in the dynamic motions of materials. This can be ascribed to the fact that there are tremendous size discrepancies (typically $10^6$–$10^9$ times difference in size) between molecules and material dimensions. In biological systems, the molecules and macromolecules (proteins) are assembled and organized in highly sophisticated and hierarchical manners to express dynamic biological functions. A great deal of efforts have been made since long to realize such structures in artificial systems, and perhaps biological systems have the greatest interest from in organic and material chemists. In reality, however, such a target is difficult to achieve with the current experimental tools

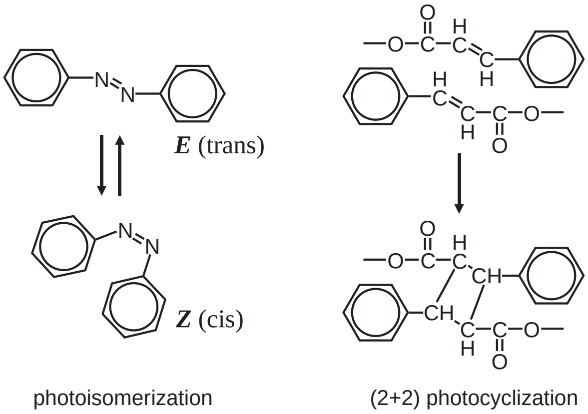

Fig. 1. Photoreacting units.

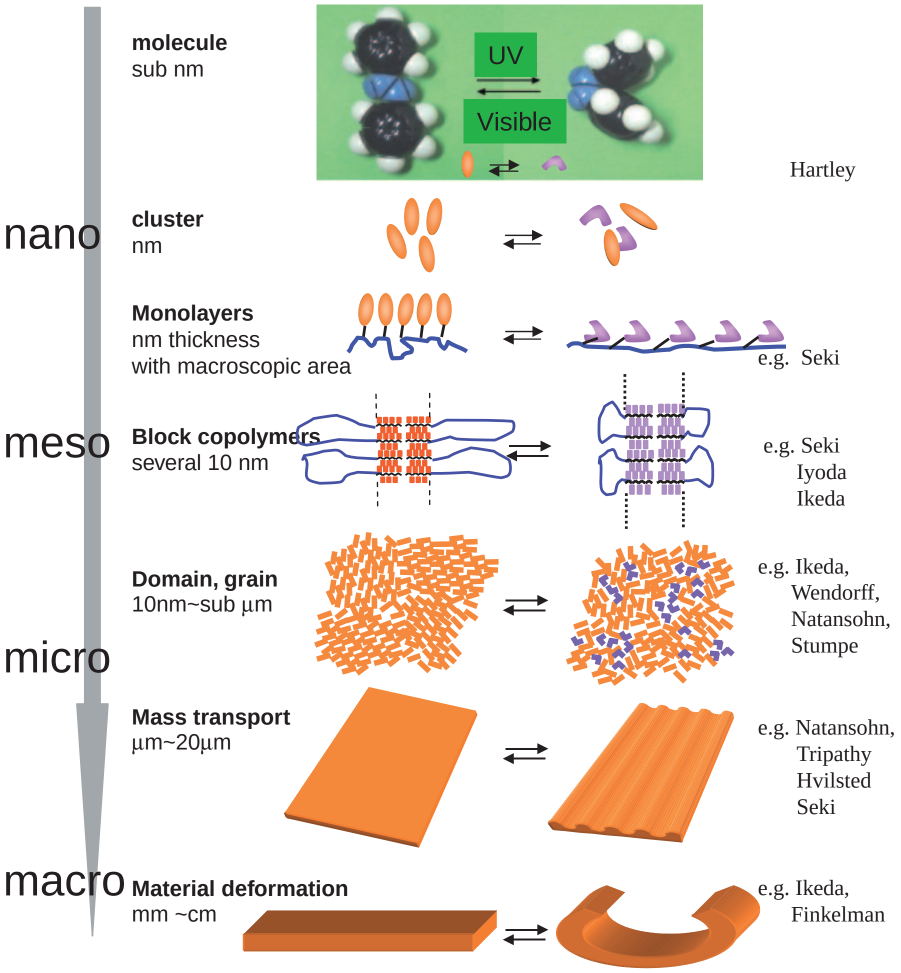

Fig. 2. Hierarchical classifications of molecule to materials for Az-containing soft film materials and representative research targets for each hierarchy.

and materials. However, we can put various phenomena in order based on the feature size and hierarchical structures and design research for individual hierarchies with some extensions.

Let us consider the hierarchies of Az-containing soft materials (Fig. 2), for example. The scheme starts from molecule (sub nanometer size) to material (typically micro- to centimeter size). In each hierarchy of nano-, meso- (2–50 nm defined by IUPAC), micro-, and finally to macroscopic sizes, typical research targets are also shown. Among them, monolayers at 2D interfaces provide alluring systems, of which the thickness is in an molecular size but the area can be extended to a macroscopic size. They can serve as favorable bridges between molecules and materials. In this respect, many of our strategies and research ideas have been based on the monolayered states. Block copolymers form mesoscopic phase separated structures by self-assembly, which have recently been of intense research targets in polymer chemistry. In liquid-crystalline (LC) materials, the molecular assembly in general forms domains typically in micrometer sizes. How to control and orient the molecular orientations is of particular significance from practical viewpoints. The phenomenon of photoinduced mass migration to form relief structure in a polymer film was discovered in 1995. In this case, migrations and transports occur on micrometer level, which can be classified into a larger sized hierarchy. Finally, photo-driven materials possessing large sizes visible to naked eyes have been developed quite recently. Of course, these are only selected examples, and many more characteristic light-driven phenomena and processes are known so far. Nevertheless, it is emphasized that materials must be understood based on the hierarchical levels in order to design new smart responsive materials.

Research on Az-containing polymeric films has exploded during the past few decades, and it is continuing to be a very active area of materials chemistry.[5–8] Azobenzene is perhaps the most frequently used photochoromic unit (Fig. 1, left) to be incorporated in molecular assemblies and organized polymeric materials. It has several advantageous features for fabrication of photoresponsive systems; i) Tedious synthesis is generally not required, leading to facile preparation of planned derivatives. ii) The sensitivity of *E* (trans)-form $\rightleftharpoons$ *Z* (cis)-form photoisomerization is moderately high for both directions for derivatives having alkyl or alkoxyl substituents. Besides, less expensive light sources, such as a Hg lamp can be used. iii) Photofatigue is negligible under ordinary laboratory conditions. iv) The molecular shape is rodlike and symmetric, which favors incorporation into various molecular assemblies especially into liquid-crystalline systems.[8–11] In the light of above facts, although the photo "chromic" function Az unit is not so important, the shape change and polarity change of the molecule to trigger motions are stressed to a much larger extent. The photophysics and photochemistry of Az has been summarized in the literature.[12,13]

Another essential key to this research is how to assemble and organize molecules and polymer materials. In organized systems, the motion of "hot" molecules can be transferred and amplified to larger scale levels of materials ranging from nanometer levels to over centimeter levels. For the Az unit, one often needs to provide efficient reaction fields in the molecular assemblies.[14–17] The understanding of the interplay between the photoreacting unit and the organized molecular or macromolecular assemblies is of essence to conduct exploration in these areas. Although only a few topics are summarized in this article, it is expected that these approaches can be extended to create new classes of photofunctional soft materials.

## 2. Photomechanical Response in Monolayer Systems

**2.1 Macro-Size Photomechanical Effects. 2.1.1 Polymer Monolayers:** In a 3D bulk state, molecular motions in response to light cannot be directly reflected in the macro-size behavior, because of structural complexities and hierarchies existing in the materials.[18] In the monolayer state, on the other hand, changes in the molecular shape and orientation can be simply and directly related to the film properties, such as film area and surface pressure. In this regard, lowering the dimensionality from three dimensions (3D) to two dimensions (2D) is particularly meaningful.

Photoresponsive effects in Az-containing polymers were first reported by Blair et al.,[19,20] who have utilized polyamide with an Az unit introduced in the main chain. Since then many attempts have been made to observe the photoresponsive behavior of monolayers on water.[21–31]

Seki et al.[32–34] have prepared poly(vinyl alcohol)s (PVA) having an Az-containing side chain (Fig. 3, 6Az*n*-PVA, *n* being the carbon number of the methylene spacer between Az and the polymer main chain) and have observed photoinduced area changes on a water surface. The magnitude of the film deformation is the function of spacer length connecting the Az moiety and the PVA backbone. Irradiation with 365 nm light brings about a rapid expansion of the monolayer. The largest effect is observed for 6Az10-PVA. The film exhibits a ca. 3-fold expansion from the original area. When 436 nm light is irradiated, the film shows a rapid contractile motion to the initial area, and it is fully reproducible (Fig. 4). This is the largest level of deformation for a monolayer system until now. The dipole moment of Az in the cis-form is much larger than that of the trans-form, which brings about a contact with the water surface. This leads to the expansion of the monolayer. The reversible process takes place upon visible light irradiation. This model is reasonably understood by dependence of the spacer length. In situ X-ray reflectivity (XR) analysis on the water surface has been performed by Matsuoka et al.[35] for 6Az10-PVA. Kiessig fringes are observed for specular measurement for 6Az10-PVA monolayers on a water surface. From analysis of the XR data, it is indicated that the thickness of the monolayer becomes larger for the trans form than that for the cis form. The thickness change by 0.2–0.3 nm due to the trans–cis configurational changes in the hydrophobic side chain is directly proven on the water surface.[35]

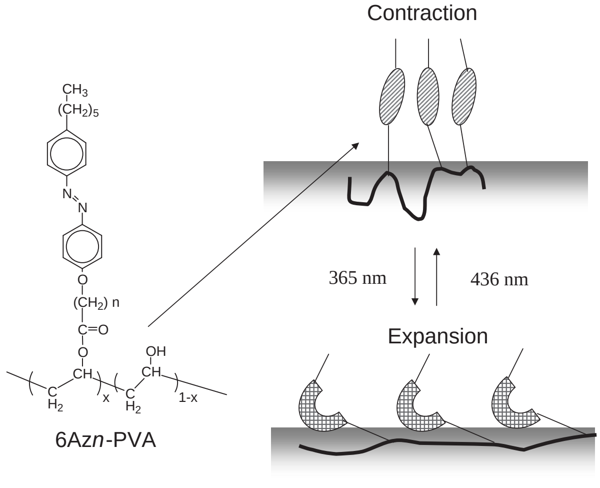

Fig. 3. Mechanism of photomechanical response in 6Az*n*-PVA monolayer on water.

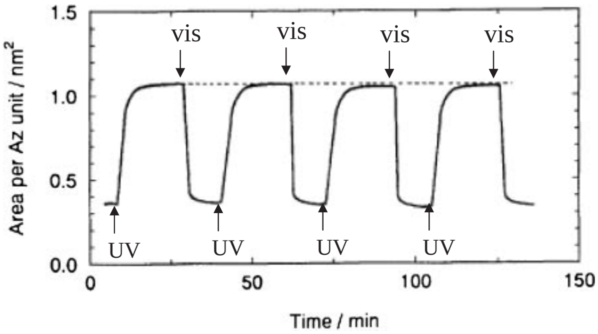

Fig. 4. Reversible photoinduced expansion/contraction responses in 6Az10-PVA monolayer [Reproduced with modifications from *Bull. Chem. Soc. Jpn.* **1996**, *69*, 2375] (Fig. 3).

**2.1.2 Supramolecular Approach Using Urea Derivatives:** Supramoleucular architecture formed through hydrogen bonding is now occupying a major research area in polymer chemistry.[36,37] It seems of value to use such material in the photoresponsive monolayer systems, instead of employing polymers. Here, urea-containing Az derivatives was adopted (Fig. 5).[38–42] Urea was chosen as the hydrophilic head, because the monolayer of alkylureas shows interesting characteristic properties attributed to the formation of so-called bifurcated (double) hydrogen bond among the urea units on water (see scheme in Fig. 6).[43–46]

When urea is connected with Az unit, further interesting behavior appears as follows: 1) Trans-to-cis photoisomerization of Az is completely quenched at the air–water interface despite the fact that the absorption maximum of the $\pi$–$\pi^*$ band almost coincides with that in solution.[38] 2) A transferred monolayer on a hydrophilic substrate shows characteristic a humidity-sensitive spectral change due to the alternating 2D packing state in a reversible manner.[47] This may provide an interesting molecular system for environmental sensors. 3) Obvious and multifarious carbon parity (even–odd) effects are observed with respect to carbon number of the spacer connecting the Az moiety and urea in both monolayers and multilayer systems as reported by Kobayashi et al.[41,42]

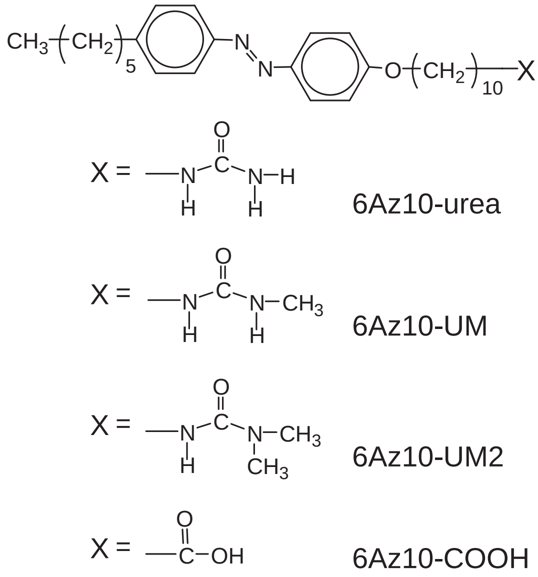

Fig. 5. Az-containing urea and carboxylic acid derivatives.

The crucial role of the bifurcated hydrogen bonding for the appearance of above features is clearly indicated by the chemical modification of urea moiety.[40] Figures 6 shows the area changes of the monolayers of 6Az10-urea, 6Az10-UM, 6Az10-UM2, and 6Az10COOH upon irradiation with UV and visible light at 20 °C and 2 mN m$^{-1}$. As seen from Fig. 6, no photoreaction and thus no photoinduced area change are observed in the 6Az10-urea and 6Az10-UM monolayers. In sharp contrast, the spectrum of 6Az10-UM2 monolayer exhibits reversible area changes under alternating irradiation. Also, the 6Az10-COOH monolayer behaves in the same manner. The discrepancy is attributed to the mode of hydrogen-bond formation, namely, the above two monolayers can form bifurcated hydrogen bonds, whereas the remaining two form only single-strand hydrogen bond (see the cartoons in Fig. 6). Also, other interesting phenomena are observed in the urea Az monolayer and multilayers.

**2.2 Visualization of 2D Motions by Microscopic Observations.** Macro-size mechanical responses at $10^{-1}$–$10^{-3}$ meter levels can be evaluated by film balance measurements. On the other hand, motions and structural changes at molecular ($10^{-9}$–$10^{-10}$ m) levels can be evaluated by absorption spectroscopy, X-ray reflectivity and surface potential measurements. Thus, there exists a tremendous scale gap between the observation tools and hierarchical structures. To bridge the two scale regimes, microscopic visualization methods are

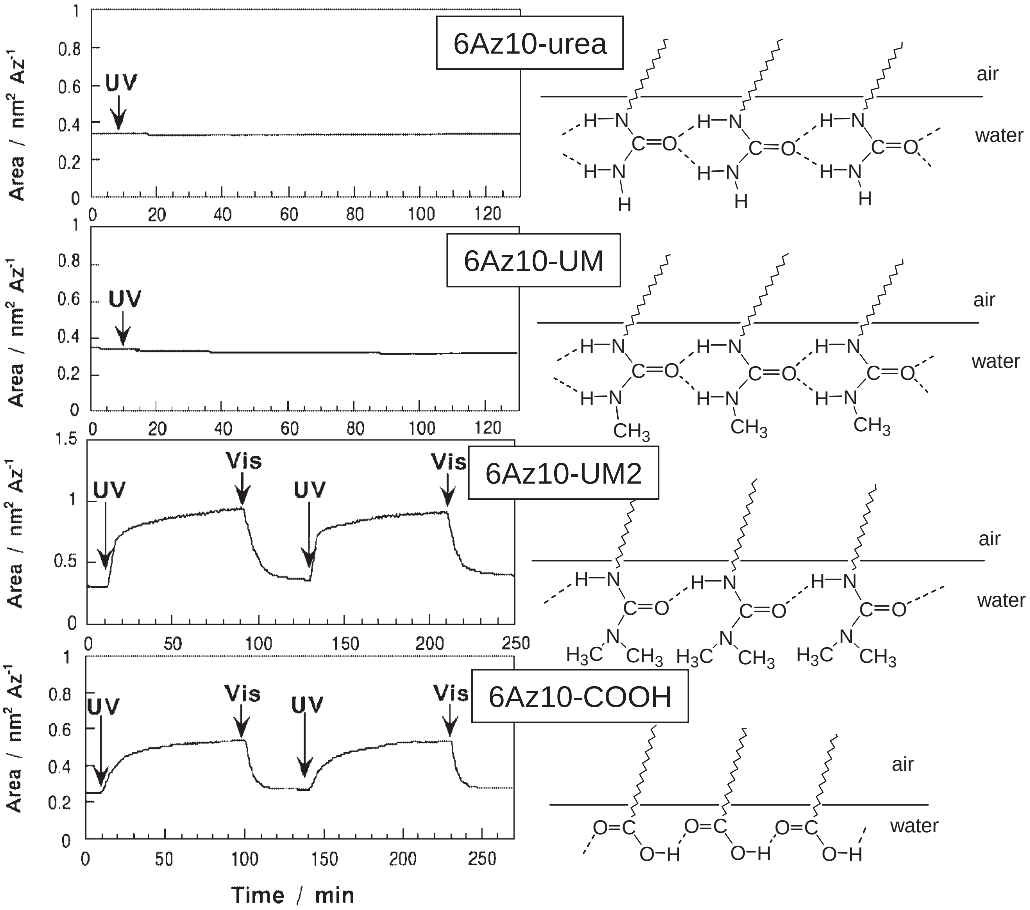

Fig. 6. Photomechanical behavior in Az-urea and carboxylic acid monolayers [Reproduced with modifications from *Langmuir* **2002**, *18*, 5462, Copyright permission: American Chemical Society] (Figs. 6 and 7).

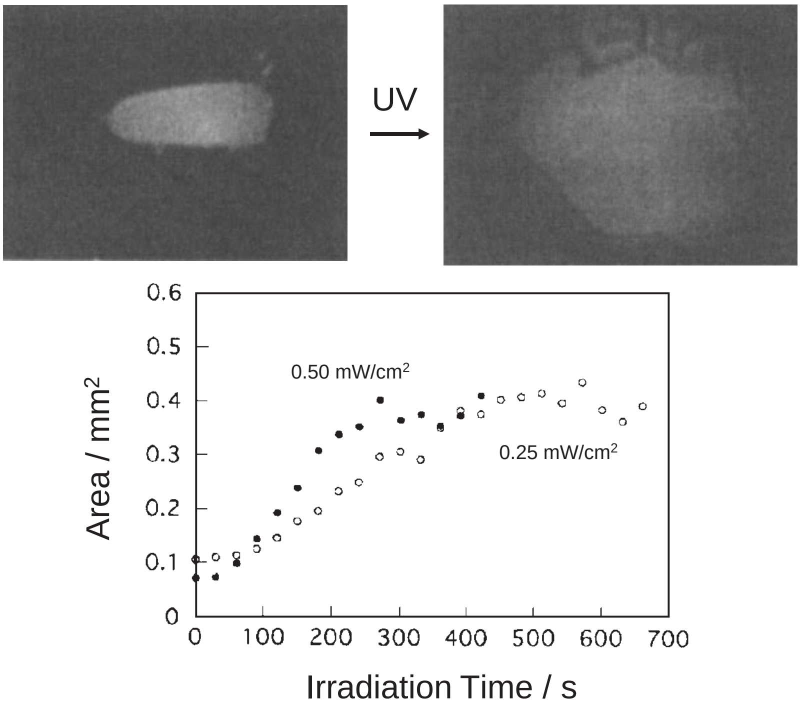

Fig. 7. Direct observation of photoexpansion of 6Az10-PVA monolayer on water by BAM [Reproduced with modifications from *J. Phys. Chem. B* **1998**, *102*, 5313, Copyright permission: American Chemical Society] (Figs. 6 and 7).

of particular importance. The dynamics of the photoresponsive monolayers has been actually revealed by visualization tools. Optical microscopic tools, such as fluorescence microscopy and Brewster angle (ellipsometric) microscopy (BAM), cover scale ranges around $10^{-3}$–$10^{-6}$ meter levels. Atomic force microscopy (AFM) visualizes smaller ranges from micrometers to molecular levels. In situ observations on the water surface, which reflects the "living" state, are feasible by the optical microscopies; however, the transfer process onto a solid substrate is required to perform AFM observations. Both methods are very important and complementary visualization tools to cover the entire scale.

**2.2.1 BAM Observations:** BAM utilizes the propagation and reflecting properties of light,[48,49] and it is well suited for observation of photochromic monolayer systems because no additional photoexcitable molecule is required. We utilized BAM to clarify the nature of photomechanical response in monolayer using 6Az10-PVA.[50,51] For these purposes, a small mobile trough that can chase an isolated piece of photoresponsive monolayer within the microscope field was constructed (Fig. 7, upper). With this setup, the photoinduced area changes with time are directly followed from the BAM image. An important observation is that an induction time is clearly observed before the monolayer starts expanding, despite the fact that the trans-to-cis photoisomerization proceeds just after the switch-on point of illumination. The expansion occurred after more than 40% of the Az side chains are isomerized to cis-form (Fig. 7, lower). This fact can be the consequence of an antagonistic action between the expanding action of cis-isomerized side chains and contracting (aggregating) effect of the trans side chains. Thus, the mechanical process involves strong molecular cooperativity. At $2\,\mathrm{mN\,m^{-1}}$, the expansion started after the monolayer system almost reached to its photostationary state. The nonlinear property in the expansion process depends on the spacer length. The longer alkylene spacer gives rise to stronger nonlinearity due to the stronger aggregation action in the trans form.[52]

**2.2.2 AFM Observations:** Large distance migrations of a polymer monolayer in relation to mechanical response are indicated with 6Az10-PVA monolayer by AFM.[53,54] It was found that the morphology of the 6Az10-PVA monolayer on a hydrophilic mica surface changes upon illumination in a highly humidified atmosphere. The motions of the monolayer are assisted by water molecules existing on the hydrophilic surface.[55,56] For sparse monolayer ($1.2\,\mathrm{nm}^2$ per Az unit), the UV light irradiation induced a 2D expansion of the layer, which then reverted to an essentially identical thermally contracted morphology after a few days. When the layer was more densely packed ($0.4\,\mathrm{nm}^2$ per Az unit), the layer showed a sponge-shaped structure with a number of defects. Upon UV light illumination, most of the defects disappeared, and huge shallow pan-like protrusions of 200–300 nm in diameter and ca. 10 nm in height appeared. This 3D change was also nearly a reversible process. The 3D protrusions probably consist of bubbles instead of multi-layering from the following facts. Matsumoto et al.[57,58] also have observed similar effects for an ion complexed monolayer formed between an anionic Az derivative and a cationic polymer.

In an extremely dilute state, the 6Az10-PVA monolayer has been isolated on the single chain level.[59] This state is realized via a process of so-called skeletonization. Skeletonization involves selective removal of one component from a mixed organization.[60,61] 6Az10-PVA was mixed with a stuffing amphiphile (oleic acid or methyl oleate), which becomes highly expanded at the air–water interface. After transfer onto a mica surface at very low pressures, the stuffing material was then removed by washing or evaporation in reduced pressures at elevated temperatures. Dot-shaped films having ca. 20–30 nm radius were obtained consequently. Volume estimations and some considerations suggest that the dot films are consisting of a single polymer chain or at least separated at a comparable level. In situ AFM measurements showed the actual expansion (after UV light irradiation) and contraction (visible light) behavior of the isolated polymer monolayer, accompanied by a thickness reduction from 1.2 to 0.5 nm, which reasonably agrees with the model shown in Fig. 3. These motions were fully reversible. A more crowded assembly also indicates fully reversible morphological changes between a completely isolated film in the trans state and continuous film formation in the cis state (Fig. 8). This fact implies that the polymer chains restricted in the 2D state cannot be entangled with each other. This reasonably accounts for the rapid separation and reproducibility of the dot structure.

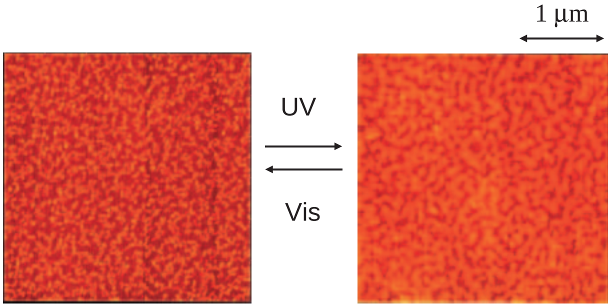

Fig. 8. Observation of photomechanical behavior in 6Az10-PVA monolayer on mica by AFM [Reproduced with modifications from *J. Phys. Chem. B* **1999**, *103*, 10338, Copyright permission: American Chemical Society] (Fig. 2).

**2.3 Modulations of 2D Nanostructures. 2.3.1 Photoresponsive Block Copolymer Monolayer:** Microphase separation (nanostructure formation) by block copolymers in thin films has been a subject of intensive study from the view point of self-assembly in confined state.[62,63] From practical viewpoints, such nanostructures also have been receiving considerable attention for fabrication of ever smaller feature sizes than those obtained by the photolithography process. They have potential applications for high-density data-storage media,[64–66] ultrafine filters or membranes,[67,68] template for metal nanowires,[69] etc.

On an aqueous surface, molecular interactions of polymer chains with water and intrinsic microphase separation properties of block copolymers both play important roles in the evolution of characteristic nanostructures. In the monolayers on water, the fractional composition of the blocks and surface pressure applied on water are the dominating parameters controlling the nanopattern features.[70–72] It is anticipated that, when one block is made of photoresponsive segment (area variable component), the change in the area fraction may alter the phase-separated nanostructures. Actually such light-induced modulations in the 2D nanostructures have been attained by Kadota et al.[73] for an ABA-type triblock copolymer, p($Az_{42}$–$EO_{202}$–$Az_{42}$), where A and B correspond to Az-containing polymethacrylate and poly(ethylene oxide) (PEO), respectively (Fig. 9). This polymer is synthesized by atom-transfer radical polymerization (ATRP), according to a modified method of Iyoda et al.[74]

The monolayer is transferred onto a freshly cleaved mica surface. As shown, the isomerization state of Az on water led to significant change in the microphase separation patterns. The morphology in the trans-Az is characterized by a mixture of dot and rod shapes. Apparently, the rod aggregates consist of lined aggregates of dots. Judging from several experiments,

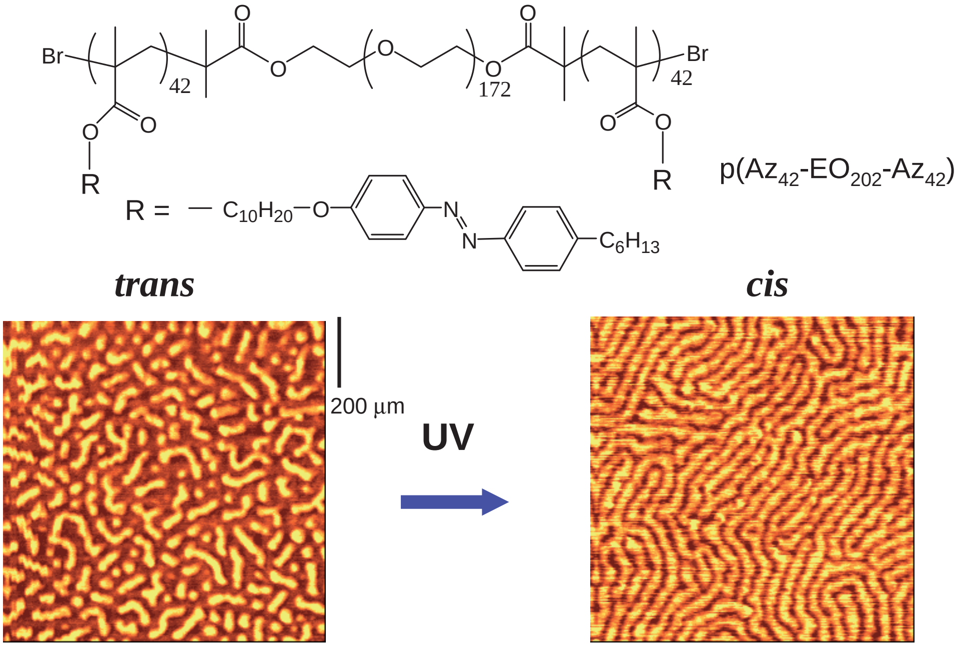

Fig. 9. Photoinduced modification of 2D nanostructures in p($Az_{42}$–$EO_{202}$–$Az_{42}$) triblock copolymer monolayer on water observed by AFM [Reproduced with modifications from *J. Am. Chem. Soc.* **2005**, *127*, 8266, Copyright permission: American Chemical Society] (Fig. 2).

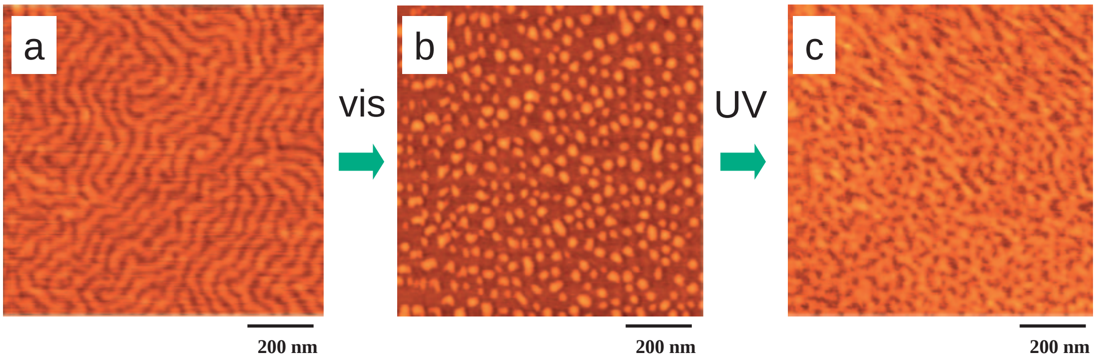

Fig. 10. Direct photoinduced modification of 2D nanostructures in p($Az_{42}$–$EO_{202}$–$Az_{42}$) triblock copolymer monolayer on mica. Initial cis-rich state (a), trans-rich state after UV irradiation (b) and successive cis-rich state after visible light irradiation (c) [Reproduced with modifications from *Colloids Surf., A* **2006**, *284–285*, 535, Copyright permission: Elsevier] (Fig. 3).

the higher domains should be composed of the Az block. Fourier transformation of the image affords the width of the rods or the diameter of dots to be ca. 30 nm. The bulky mesogenic unit of Az in the side chain should impede the conformational flexibility, leading to an almost fully stretched chain.[75] The monolayer in the cis-Az gives characteristic elongated branched flat stripe patterns maintaining the ca. 30 nm widths. The almost fully stretched polymer chains of the Az block are oriented perpendicular to the domain interface. Thus, upon UV light illumination, the cis-isomerized Az side chains contacts with the water surface orienting parallel to the interface, resulting in the characteristic anisotropic microdomain expansion parallel to the rod-shaped domain. This behavior is in contrast to the case of the homopolymer, in which only simple 2D uncontrolled expansion occurs.[51]

The alternating 2D nanostructures was also observed on a solid surface (Fig. 10).[76] When the p($Az_{42}$–$EO_{202}$–$Az_{42}$) monolayer deposited in the cis form (a) was irradiated with 436 nm light (2 mW cm$^{-2}$ for 30 min), the elongated stripe microphase separation structure became a clear dot morphology with an increased height difference (b). When UV light was irradiated successively, the morphology reverted to the flat patterns with quasi strip features (c). Thus, the stripe/dot reversible 2D changes are induced by light when the illumination is performed starting form the monolayer in the cis form.

For ABA triblock copolymers, the B block (the center chain) adopts, in general, a mixture of bridge and loop conformations in the 3D bulk. If the bridge conformation exists in the present 2D system, the structure of the microphase separation will not be altered. Thus, almost all B chains (PEO) in the monolayer should adopt the loop conformation. Together with the knowledge of the width of the stripe and diameter of the dot structure, one can assume that the stripe and dot patterns are comprised of a bilayer structure and flower-micelle-like 2D aggregates. The dominant population of loop conformations coincides with the tendency of segregations rather than interpenetration of polymer chains in the 2D state.[59,77,78]

**2.3.2 Ordered Morphology Induction in Block Copolymer Monolayers:** When an amphiphilic block copolymer is spread on water with a highly volatile solvent, the hydrophobic blocks immediately aggregate to form surface micelles. These surface micelles exhibit various surface nanostructures governed by various parameters, such as physical and chemical characteristics of blocks (amphiphilic nature, solubility, molecular weight, block size, etc.) and processing factors (solvent used, concentration of spreading solution, temperature, compression speed, etc).[79–83] The resulting surface nanostructures of such conventional spreading method contains dissipative factors in large parts. To obtain ordered nanostructures of surface micelle at macroscopic regions, spreading conditions must be customized.

Fully hydrophobic polymers consisting of only hydrocarbon side and main chains cannot be spread as a monolayer on water[84–86] due to the lack of affinity to water.[87] In contrast, Nagano et al. have successfully prepared ideally spread monolayers of fully hydrophobic polymers on water with the assistance of a polar liquid crystal (LC) molecule, 4′-pentyl-4-cyanobiphenyl (5CB).[88,89]

This method was applied to a diblock copolymer, polystyrene-*block*-poly(4-vinyl pyridine) (PS–P4VP).[90] The pure PS–P4VP film at 0.6 nm$^2$ (before pressure increase) exhibits heterogeneous morphologies containing both dot-like particles and ribbons. The particles correspond to the core aggregates of the hydrophobic PS parts, and the surface micelles form concurrently with spreading on water. On the other hand, no aggregate feature of PS parts was observed in the same area conditions when spread with 5CB. A molecularly flat film was first obtained before compression (Fig. 11a). This homogeneous and smooth surface suggests that hybridization with LC prevents the aggregation of the PS part, yielding a spread monolayer of the fully hydrophobic PS block. When the pressure was increased, regularly sized dots started to appear (e.g., 1 mN m$^{-1}$, Fig. 11b). With further compression, the number of PS dots increased, and then the size and arrangement of dots became more and more regular. At 4 mN m$^{-1}$, perfectly ordered hexagonal dot array appeared in the PS–P4VP/5CB hybrid film on a water surface (Fig. 11c).

The monomolecularly smooth and homogeneous film shown in Fig. 11a is worth pointing out. Interestingly, no microphase-separated structure was observed with both topological and phase-mode of AFM measurements, indicating that an ideal hybridization with 5CB is attained without any phase separation of PS–P4VP blocks as well as aggregation of hydrophobic PS parts. Here, 5CB monolayer behaves as a “monolayered solvent.” The more important factor is that this “solvent” is not volatile on water. The hydrophobic PS chains

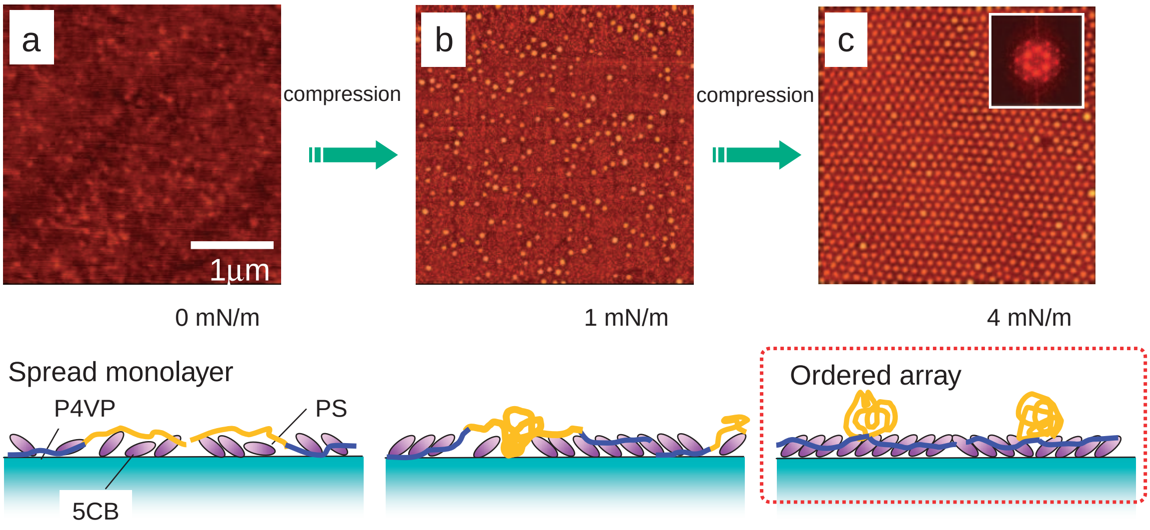

Fig. 11. Morphologies of PS–P4VP/5CB hybrid 2D assemblies on water observed by AFM [Reproduced with modifications from *Langmuir* **2006**, *22*, 5233, Copyright permission: American Chemical Society] (Figs. 2 and 4).

of the PS–P4VP/5CB monolayer will more readily collapsed in the compression process than the polar P4VP chain due to the less stabilization on water. 5CB, which behaves as a 2D solvent, plays an important role in equilibrating the system, bring about the formation of regular ordered dot array. The advantage of this method is that it provides highly ordered structure over large areas with high reproducibility.

5CB molecule can be readily removed from the hybrid film by simply dipping in cyclohexane. Figure 12 depicts the UV absorption spectra of the PS–P4VP/5CB monolayer on a quartz substrate before (dotted line) and after (solid line) dipping into cyclohexane for 5 min. The absorption at 280 nm corresponds to the $\pi$–$\pi^*$ transition of 5CB molecule in the hybrid film. The UV spectrum after the dipping treatment showed no trace of the absorption ascribed to 5CB, indicative of perfect removal of 5CB molecule from the deposited monolayer. To our surprise, the ordered dot array on the mica substrate is fully retained after the identical procedure. In other words, 5CB is essential for promoting the highly regular nanopatterns; yet, it is instantly removed when applying the patterns to practical uses. It is anticipated that, by introducing photoresponisve units in the polymer or in the 2D solvent, more sophisticated smart photoresponsive systems will be created.

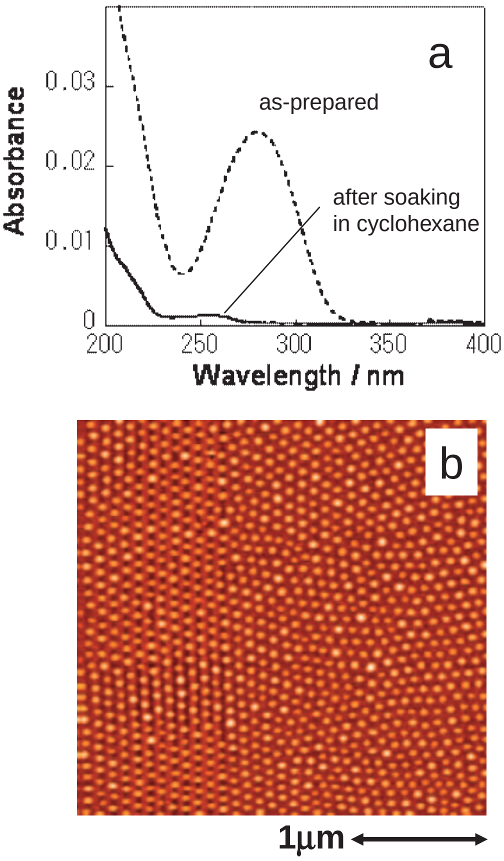

Fig. 12. Removal of 5CB from the PS–P4VP/5CB hybrid 2D assembly. UV–visible spectral change upon immersion in cyclohexane (a) and topological AFM image after removal of 5CB [Reproduced with modifications from *Langmuir* **2006**, *22*, 5233, Copyright permission: American Chemical Society] (Fig. 3).

## 3. Surface-Mediated Control of Functional Materials on Photoresponsive Layers

The surface-mediated photochemical alignment switching of nematic LCs on an Az-containing monolayer (command surface) was first reported by Ichimura et al.[8,91,92] The application to LC systems is the earliest and widely examined example of the surface-mediated photocontrol[8,93] and perhaps provides the most smart and practical systems due to the highly cooperative assembling nature of these anisotropic fluid matter. This section introduces our attempts to photoalign-organized materials other than typical LCs, namely, polymer thin films and mesoporous silica. The first attempt was initiated by replacing nematic liquid crystals with polymer thin films.

**3.1 Conformational and Orientational Control of Polysilane Films.** Light-triggered alignment of a polysilane has been initiated by Fukuda et al.[94–96] A polysilane is employed due to its versatile optical properties, namely the strongly light-absorbing properties attributed to the $\sigma$-electron conjuga-

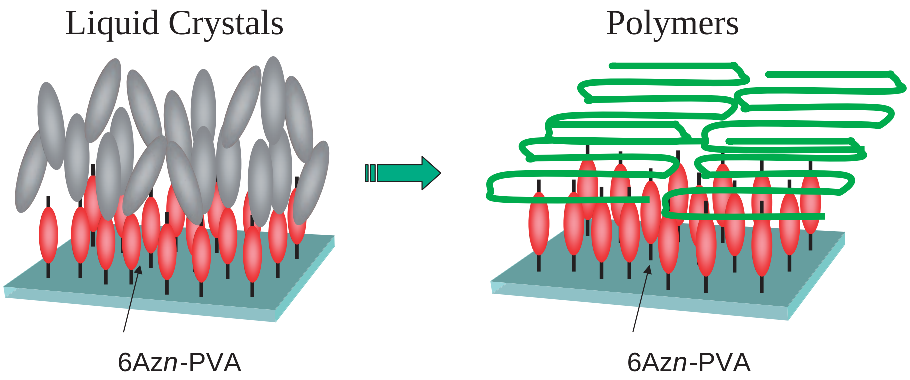

Fig. 13. Command surface for nematic LC (left) and polymer film (right).

tion.[97] The absorption property is strongly dependent on the backbone conformation and orienting direction that is parallel to the backbone extension. Poly(di-*n*-hexylsilane) (PDHS) is particularly suited since the optical properties coupled with the conformational state have already been well investigated.[97]

A spincast film of PDHS (ca. 60 nm thickness) was prepared on a 6Az10-PVA monolayer (Fig. 13). The crystallization process after casting can be readily monitored from the spectral change. The crystallization rate was accelerated on the cis-Az monolayer and retarded on the trans-Az monolayer.[94] Most probably, the nucleation process at the interface between the PDHS film and the Az monolayer is altered by the photoisomerization, which then results in the crystallization control of the whole film, meaning that the photoresponsive molecular surface can control the physical state throughout the entire thickness of the polymer film.

A vast amount of investigations on photoalignment of LCs have been reported during the last one and a half decades. Irradiation with linearly polarized light (LPL) induces photoinduced anisotropy, in which molecules are generally oriented to an unexcitable direction, namely, perpendicular to the electric vector of the polarization direction. This effect is called photoinduced optical anisotropy (see top cartoon of Fig. 14).[5,8–10,93] Such photocontrol becomes particularly effective in relatively viscous molecular organized media, such as polymeric LCs[98–100] and LB films.[92,101] Optically induced surface anisotropy in the Az polymer films has been successfully transferred to the orientation of various types of LC materials, widely investigated by Ichimura et al., including thermotropic chiral nematic[102] and discotic LCs,[103] lyotropic LCs,[104] and also side chain liquid crystalline polymers.[105]

Exposure of the 6Az10-PVA monolayer to LPL induces an in-plane orientation of the Az side chain as stated above. A spincast film of PDHS was subsequently prepared onto this photooriented Az monolayer. After crystallization, the PDHS film exhibited a strong in-plane optical anisotropy, as shown in the middle scheme of Fig. 14.[94,95] The polarized absorption spectra shows that the Si backbone is highly aligned perpendicular to the polarization plane of the actinic light. The aligned direction of the PDHS main chain agrees with that of the Az orientation on the substrate. The crystallization of the PDHS chain occurs on the photo-oriented Az monolayer in an epitaxial manner.

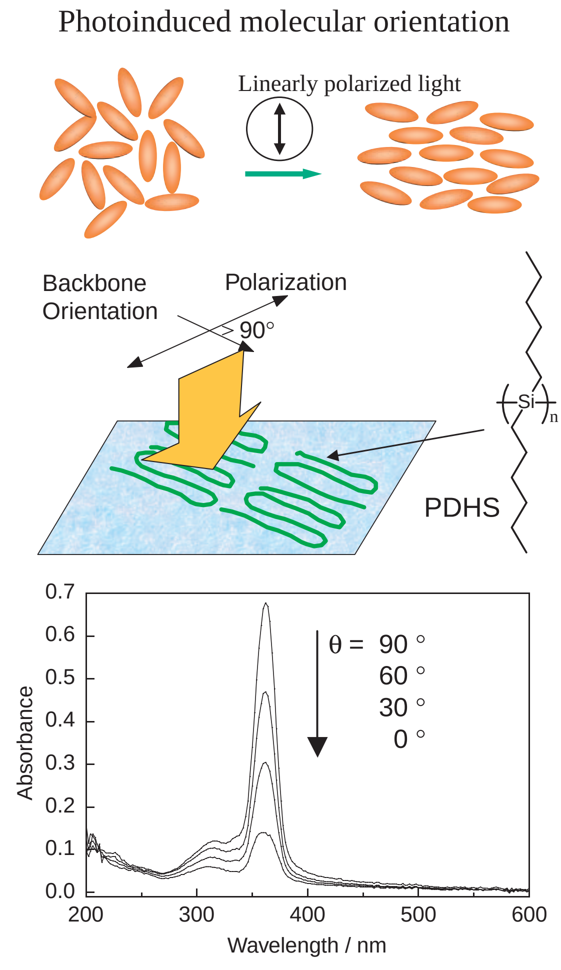

Fig. 14. Photo-alignment of polysilane via 6Az10-PVA monolayer irradiated with LPL [Reproduced with modifications from *Langmuir* **1999**, *15*, 5098, Copyright permission: American Chemical Society] (Fig. 3).

As expected, this phenomenon depends on the thickness of PDHS film. The orientational order of the PDHS backbone becomes higher for the thinner films. Effective control is available for films thinner than ca. 30 nm,[95] which coincides with the region of so-called ultrathin films where the thickness is comparable to the coil dimension of a single polymer chain.[106] When the molecular weight is in the range of ten thousand, the order parameter is enhanced after another cycle of annealing

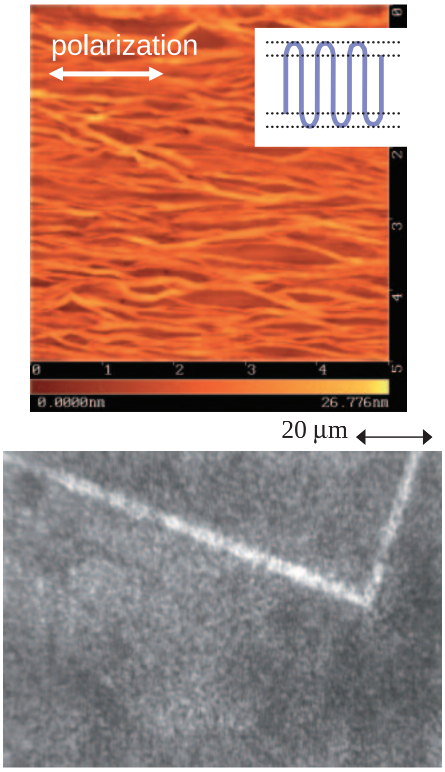

Fig. 15. AFM (upper) and polarized optical microscopic image (bottom) of photoaligned PDHS thin film [Reproduced with modifications from *Macromolecules* **2002**, *35*, 1951, Copyright permission: American Chemical Society] (Fig. 8).

and crystallization. For PDHS with molecular weight in the range of billions, the photoalignment is largely suppressed.

The length of tail part is anticipated to influence the order of photoinduced anisotropy, because the Az monolayer is anchored to the hydrophilic substrate surface via the polar PVA backbone and the tail part is positioned to the outermost surface. Thus, PDHS should interact directly with the tail part of the Az side chain. Thus, the tail length (carbon number) was varied from 2 to 12.[96] The photoinduced dichroic ratio (DR) of Az monolayers and the order parameter of PDHS gave the largest values for the Az monolayer having a $C_8$ tail.

Figure 15 shows a topographical AFM image of the photooriented PDHS and a polarized optical microscopic image of a locally photoaligned PDHS film for a thicker film indicated as a bent line. For liquid crystals, only the molecular orientation is significant. In contrast, for polymer films, the morphologies can be also a matter of interest in addition to the orientation. In the AFM image, fibrous morphologies were observed in parallel to the polarization direction of the irradiated light, whereas the direction of the main chain of PDHS was orthogonal to it. Together with the transmission electron microscopic (TEM) observation, it is implied that the main chain of PDHS is folded to form edge-on type lamellae as schematically shown in the inset of the AFM image. In the polarized microscopic image, rotation of the crossed polarizers shows appearance and disappearance of the line every 45°. This fact indicates that the bright line area is birefringent and the PDHS chains are uniaxially aligned. The dark parts are always dark by rotation, indicative of the random orientation of the polymer at micrometer levels. Thus, the micro-patterning of polymer alignment at 6 μm resolution can be achieved.[96] In the photoprocess, basically any patterned shape is applicable. Thus, local orientations of polymer chain can be produced.

### 3.2 Photo-Orientation of Mesochannels.

**3.2.1 Approaches and Materials:** Attempts have also been made to control the orientation of mesochannels of inorganic materials, which are synthesized through the sol–gel condensation in the presence of templates of rod micelle aggregates of surfactant.[107,108] Mesoporous materials are usually obtained as powders. However, recent efforts have been made to prepare thin films. Among them, Miyata and Kuroda[109,110] have reported the uniaxial alignment of mesoporous silica film deposited on a rubbed polyimide[109] or an LB film.[110] If such surface-mediated alignment is applicable also by means of a photochemical process, one can easily micro-pattern the alignment of mesochannels.

The first demonstration was performed by Kawashima et al.[111,112] In this attempt, the photoorientation of the Az monolayer is first transferred to a photoorientated spincast film of PDHS as mentioned above, and then deposition of mesoporous silica film is performed (Fig. 16, left). This 6Az10-PVA/PDMS system has weak points from following practical viewpoints: i) The process is complicated and demands handling skills. ii) The orientation of composite film does not survive temperatures above 40 °C; therefore, the structure of channels lacks mechanical stability due to insufficient crosslinking of the siloxane condensation. To overcome above problems, Fukumoto et al.[113–115] have proposed a new versatile photoalignment method using a photo-crosslinkable side-chain-type polymer with LC nature (PPLC), poly6-(4-(4′-methoxycinnamoyloxy)biphenyloxy) hexylmethacrylate, developed by Kawatsuki et al.,[116,117] in which the mesogenic biphenyl group is combined with a cinnamoyl terminal (Fig. 16, right). In many types of photo-crosslinkable polymers, an optical anisotropy of angular selective (2 + 2) photodimerization between two cinnamoyl groups undergoes using LPL.[118–120] For PPLC under investigation, the photoinduced orientational anisotropy of the film is largely amplified through self-assembling nature of liquid crystal by annealing. Another advantage of using the photo-crosslinkable polymer as the PPLC is that the resultant photochemical crosslinking firmly fixes the anisotropic molecular orientation. This feature is anticipated to allow facile performances of siloxane condensation at higher temperatures without damaging the alignment polymer film.

**3.2.2 Structural Characterizations of Mesochannels:** In the optical microscopic images of the deposited mesostructured surfactant/silica hybrids, uniaxially aligned elongated particles with widths of a micrometer range were observed. Each particle is highly oriented parallel to each other with the longer side of silica particles parallel to the polarization plane of the actinic LPL. A PDHS film surface without exposure to LPL yielded round and spherical silica particles with no preferential orientation. The effect of photo-irradiation on the morphology of the deposited silica is obvious.

Mesoporous silica can be obtained after removal of the organic surfactant template from the composite.[107,108] The surfactant molecules are generally removed by calcination by

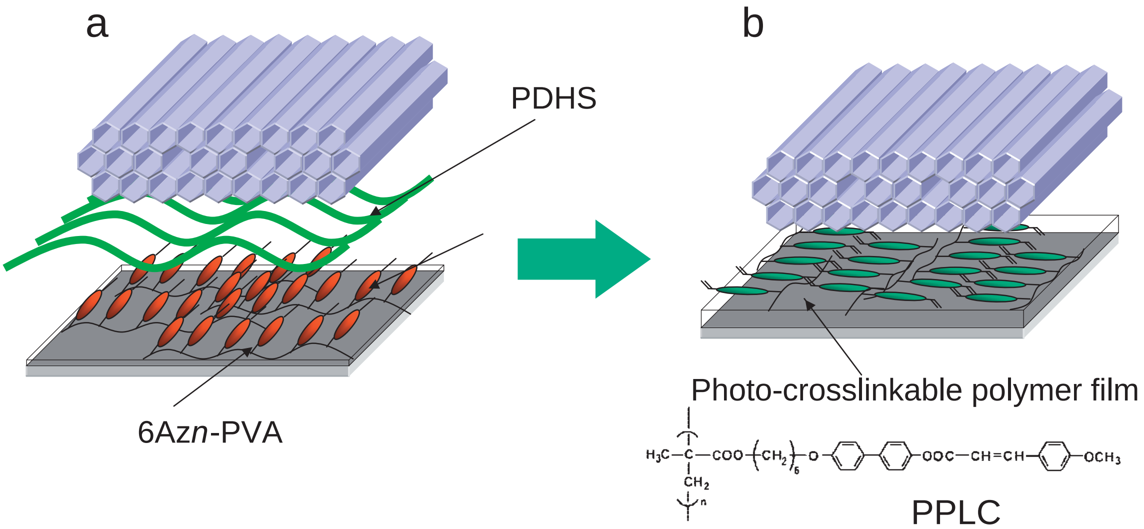

Fig. 16. Photoalignment of silica mesochannels by photoreactive polymer layers based on the photoisomerization (a) and photocyclization (b).

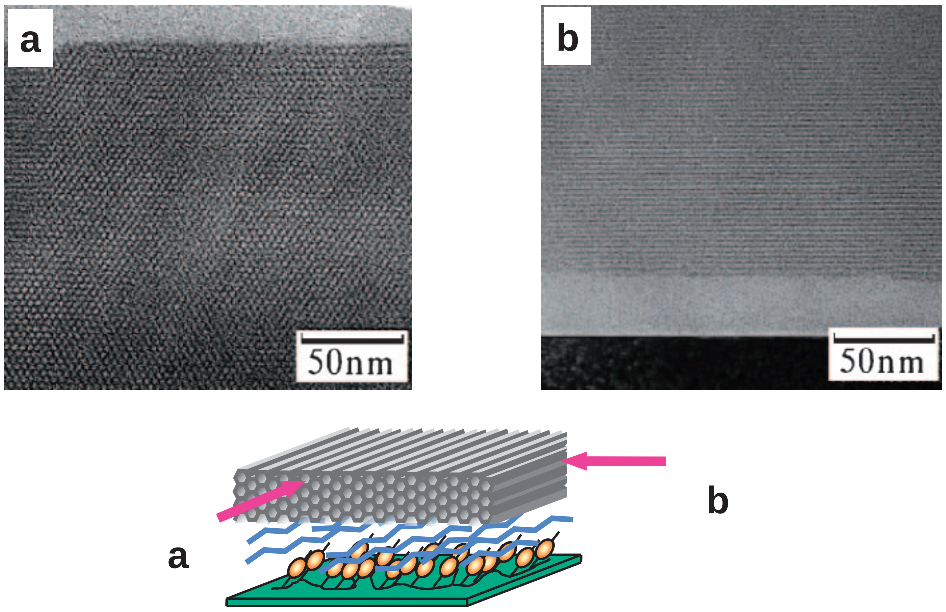

Fig. 17. TEM image of photoaligned silica mesochannels. a and b indicate the directions of observation [Reproduced with modifications from *J. Mater. Chem.* **2004**, *14*, 328, Copyright permission: Royal Chemical Society] (Fig. 6).

heating up to high temperatures exceeding 573 K. Here, photodecomposition (photocalcination) by vacuum UV light achievable at room temperature was applied according to a modified method of Hozumi et al.[121] It is expected that the distortion of the mesoporous structure in this method is more suppressed than that obtained via decomposition by heating.

The complete removal of the organic template surfactant can be confirmed by Fourier transform infrared spectroscopy for a photoaligned composite film synthesized on a silicon wafer.[112] Before the photo-decomposition of organic components, the symmetric and asymmetric bands of $CH_2$ and $CH_3$ stretching were observed in the range of $2840–2970\,cm^{-1}$, and the Si–O stretching band around $1070\,cm^{-1}$ was essentially unchanged, indicative of the retention of siloxane network structure.

Conclusive evidence for the formation of uniaxially aligned mesochannels was obtained by transmission electron microscopy (TEM) for the photoaligning layer of 6Az10-PVA/PDHS.[112] The two TEM photographs in Fig. 17 depict the cross-sectional structure of the as-synthesized surfactant/silica hybrid film observed in the two directions orthogonal to each other. Figure 17a shows the image when the film is sliced parallel to the direction of the actinic polarized light. The hexagonal structure of the mesochannels is clearly visualized through overall thickness of the film. On the other hand, when the film is sliced perpendicular to the direction of the actinic polarized light, the lines with a periodicity of 3–4 nm running parallel to the substrate are observed (b). The periodic length coincides well with that of the hexagonal spacing obtained by XRD. The cylindrical structure of the mesochannels is fully stretched

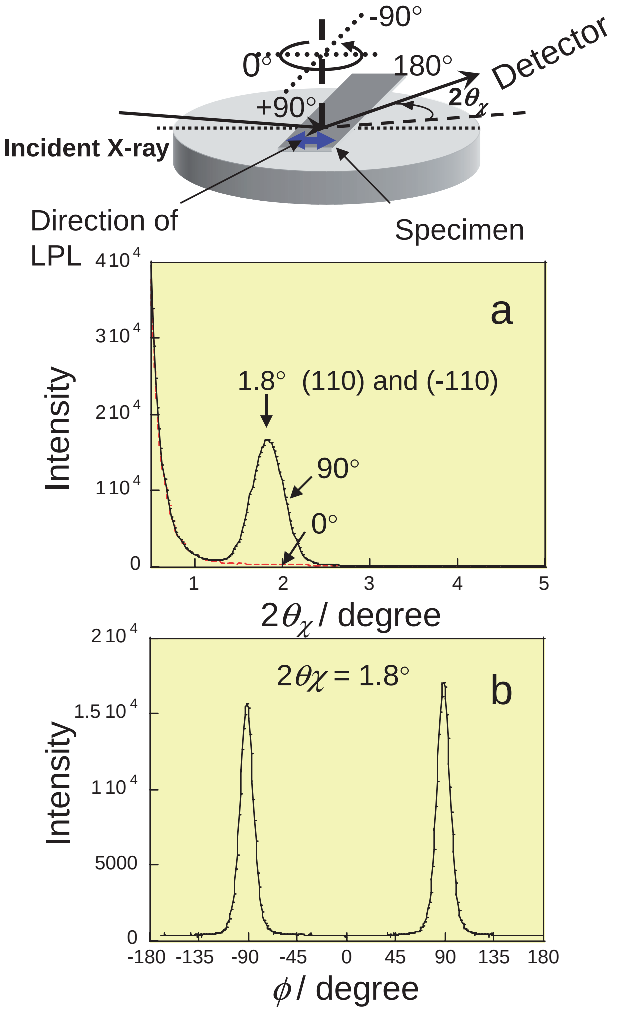

Fig. 18. In-plane XRD measurements to evaluate the photoalignment of mesochannels [Reproduced with modifications from *Chem. Mater.* **2002**, *18*, 1226, Copyright permission: American Chemical Society] (Fig. 8).

straight in the film. Figure 17 shows the hetero-interface regions composed of the Si wafer (the dark region at the bottom), Az monolayer (2 nm thickness, not clearly shown), PDHS film (40–60 nm thickness, brighter region) and deposited mesochannels with parallel stripes. The orientational information possessed by the Az monolayer is transferred to the alignment of PDHS with a thicknes of ca. 50 nm thickness and then to mesostructured channels with a thickness of ca. 400–500 nm thickness. Thus, great amplifications are attained.

The uniaxially aligned honeycomb mesochannel structure attained in macroscopic areas can be supported by the X-ray diffraction (XRD) patterns. An example is shown in Fig. 18 for a cetyltrimethylammonium (CTAC)-templated mesostructured channels aligned by PPLC polymer film.[115] The polarization direction of the LPUV light irradiated to the film coincides with parallel direction of incident X-ray at $\phi = 0°$. Figure 18b shows $\phi$-$2\theta_\chi$ XRD scan profiles of the as-synthesized mesostructured CTAC/silica composite thin film. At $\phi = 0°$, the $2\theta_\chi$ XRD signal was not observed. When the sample was rotated to $\phi = +90°$, strong diffractions at $2\theta_\chi = 1.8$ and 3.4–3.8° assignable to (−110) and (110) lattice plane perpendicular to the substrate, respectively, were observed (a). These results indicate that the mesochannels are photoaligned perpendicular to the polarized direction of the irradiated linearly polarized light. This situation is schematically illustrated in Fig. 16b. Next, in-plane rotation ($\phi$) of the silica thin film was conducted with a retention of $2\theta_\chi = 1.8°$ (b). In the −180 to +180° rotation, two obvious diffraction peaks with very narrow directional distribution were observed at $\phi = -90$ and +90° (b), indicating that the photo-oriented mesochannels have a preferential orientation perpendicular to the polarized direction of the LPL.

**3.2.3 Dipping Method:** Dip-coating was found to be also applicable.[115] In Fig. 19, in-plane XRD profiles of the CTAC/silica composite films prepared by the dip-coating are depicted. In the measurements, the direction of incident X-ray at $\phi = 0°$ coincided with the parallel direction of the dip-coat (lifting) direction (see Fig. 18). PPLC was irradiated with LPL parallel (//) and perpendicular (⊥) to the dip-coating direction. In the same manner, a scan profile of in-plane rotation ($\phi$) was obtained at $2\theta_\chi = 1.8°$. When polarized direction of the irradiated LPL is set parallel (//) to the lifting direction, two sharp diffraction peaks were observed at $\phi = -90$ and +90° (b). In contrast, when the polarized direction was set perpendicular (⊥) to the lifting direction, the diffractions were observed at $\phi = 0$ and ±180°. These facts clearly indicate that the mesochannels are aligned to the polarized direction of the LPL. It is stressed here that the channel orientation is predominantly controlled by the direction of photoaligning polymer layer and not by the lifting direction. The orientation degree of mesochannels is dependent on the thickness of the silica thin film. The thinnest film (thickness: 40 nm) had the highest order of orientation of the mesochannels. More effective photo-alignment can be achieved for the thinner film. These facts unequivocally indicate that surface-mediated transcription was attained from the molecular orientation of the PPLC film to the surfactant rod-like aggregates.

**3.2.4 Photopatterning:** Micropatterned illumination of the PPLC film with LPL was achieved, and the morphology of the resulting silica film was observed by optical microscopy (Fig. 20).[113,115] The PPLC film was irradiated with the LPL through a photomask and annealed. In the irradiated areas, linear cracks evolved, of which the direction ran perpendicular to the polarized direction of the LPL. In contrast, grain morphologies were observed in the unilluminated areas. These morphological features strongly suggest that local alignments of mesochannels are attained in the geometry of the photomask. The patterning resolution in this experiment was ca. 10 µm.

**3.2.5 Polymerization in the Photoaligned Mesopores:** Utilizing the photoaligned mesochannels, preparation of nanofibers via radical polymerization was attempted.[122] The photopolymerizable monomers, which consisted of a mixture of UV curable LC molecules, are shown in Fig. 21. It is anticipated that the monomers align uniaxially by the liquid-crystal nature in the channels and that the resulting polymer provides information on molecular orientation. Moreover, the packing state of monomers is retained during the polymerization for these monomers,[123,124] which should be of help for evaluating

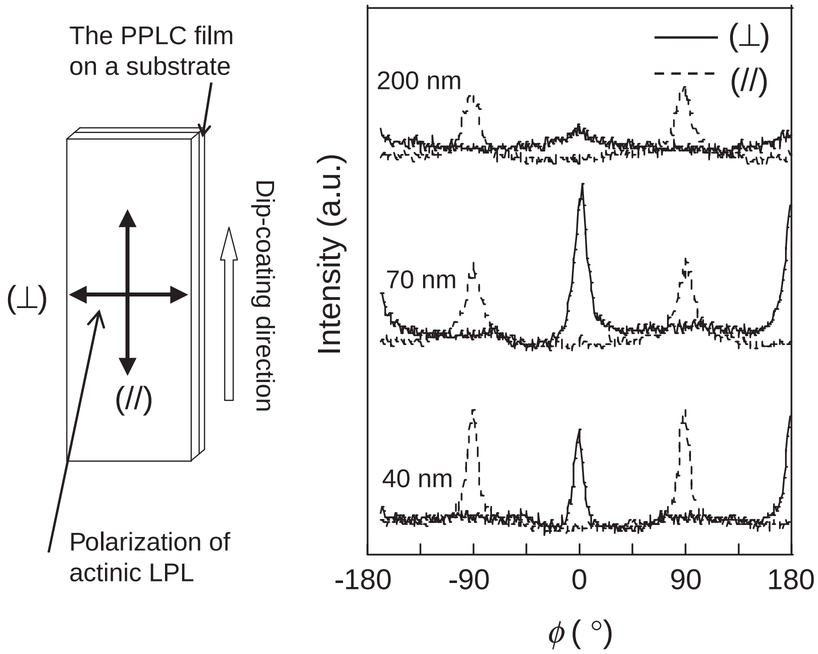

Fig. 19. In-plane XRD data of photoaligned mesochannels prepared by dipping method [Reproduced with modifications from *Chem. Mater.* **2002**, *18*, 1226, Copyright permission: American Chemical Society] (Fig. 10).

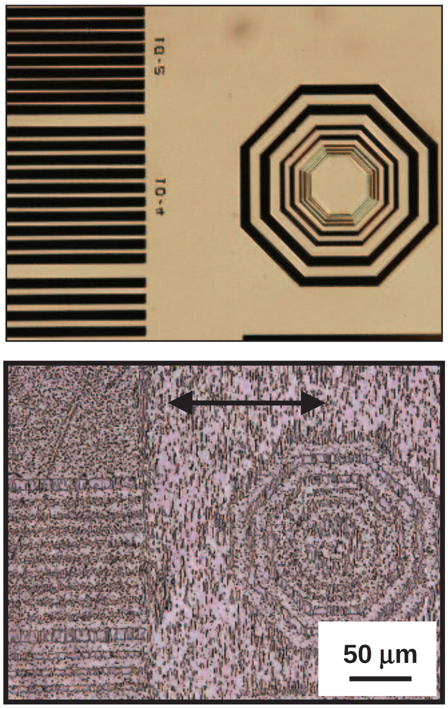

Fig. 20. Patterned photoalignment of mesochannels using a photomask. Photomask (upper) and the obtained silica film (lower) [Reproduced with modifications from *Chem. Mater.* **2002**, *18*, 1226, Copyright permission: American Chemical Society] (Fig. 11).

the molecular orientation and morphological observations. A mesostructured hybrid silica templated with CTAC film was subjected to irradiation with ultraviolet light (185 and 245 nm) at room temperature for 1 h under an $O_2$ atmosphere (i.e., $O_3$ oxidation process[125]), and a mesoporous silica thin film was obtained. The UV curable LC monomer containing a photoinitiator was inserted into the hydrophobized mesochannels under reduced pressure. In situ photo-polymerization of the LC monomer was achieved by irradiation with UV (365 nm) light.

Figure 21a shows polarized optical microscopic images of surface for the silica film after the in situ photo-polymerization placed between two crossed polarizers. When the silica film was rotated from 0 to 45° in plane, the dark image became brighter except for the crack areas. This indicates that mesogenic moieties of the molecules polymerized in the mesochannels are aligned in one-axis direction. Polarized UV absorption spectra of this film are shown in Fig. 21b. The optical absorption axis of mesogenic units was aligned preferentially parallel to the mesochannels of the silica film. The features of the polarized spectra before and after photo-polymerization scarcely changed, indicating that the orientation and the packing state of LC molecules are fixed without appreciable change after polymerization.

To extract the polymer products from the channels, the silica network was dissolved by soaking the composite in a hydrofluoric acid (HF)/ammonium fluoride buffer solution. The morphologies of the resulting polymer product observed by AFM indicate that straight bundles of nanofibers are formed (Fig. 21c). The height profile of the bundle exhibits the existence of nanometer-scale steps, strongly suggesting the formation of nanofibers by templating the mesopores with a diameters in the range of 3–4 nm diameter. Interestingly, the molecular weight control is effectively attained and the distribution of the polymer synthesized within the mesochannel became markedly narrower than that obtained via bulk polymerization.

## 4. Photo-Triggered Highly Efficient Mass Migration

This section describes another attractive characteristic of the smart phenomenon, photo-triggered highly efficient mass mi-

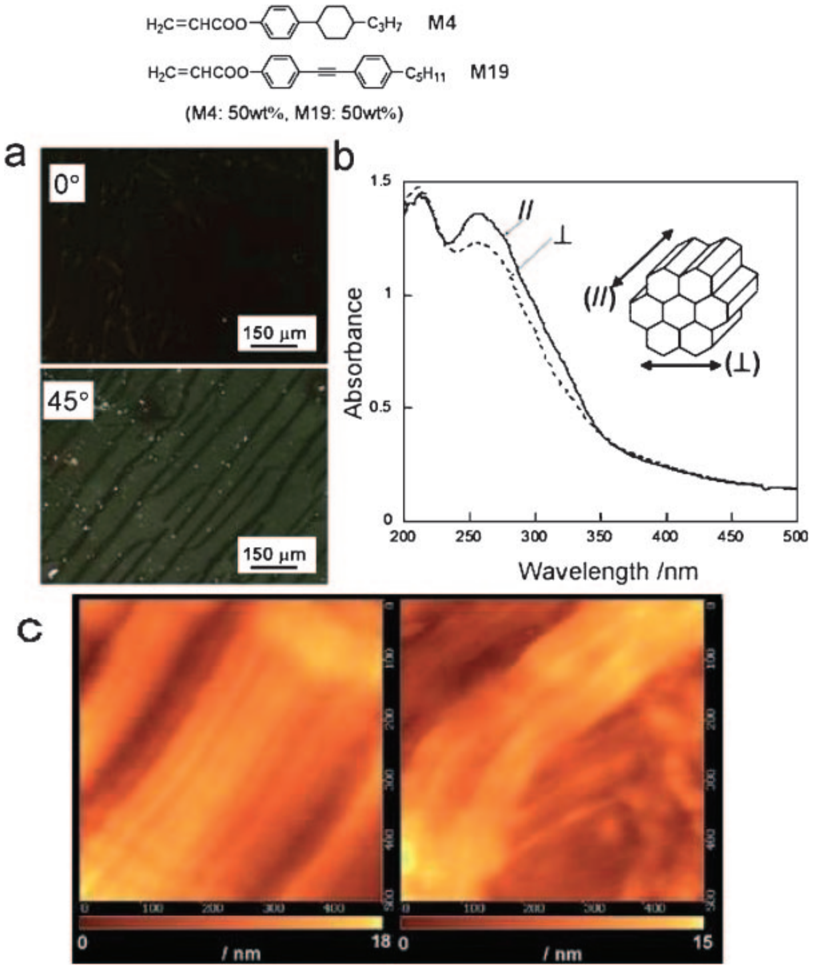

Fig. 21. Polymerization of UV curable LC monomers in photoaligned mesoporous channel. Polarized optical microscopic image (a), polarized absorption spectra (b), and obtained nanofibers (c) [Reproduced with modifications from *Chem. Lett.* **2006**, *35*, 180] (Figs. 2 and 3).

gration, which occurs as a consequence of strong and dynamic molecular cooperativity (Fig. 22). Az polymers are potentially useful as materials for reversible holographic information storage and photonic devices.[126–130] Surface relief gratings (SRG, regular topological surface modification) formed via irradiation with an interference pattern of coherent light have been demonstrated recently[131–133] and is perhaps the most interesting target in the current research of Az polymers. A great deal of data has been accumulated rapidly due to its basic phenomenological interest[134–140] and its technological applications.[138,139] This process has particular technological advantages in view of relief formation: i) it offers a facile, all-optical and single step fabrication process that does not require a wet development procedure, and ii) the surface topology is erasable by application of circularly polarized light or heating above glass transition temperature ($T_g$), which makes the process repeatable. It is of no doubt that the SRG is formed via large-scale polymer chain migration; however, the precise mechanism is still a subject of intensive investigation.

Earlier works are mostly devoted to inscription of gratings using interference light beams, and thus, the phenomenon has frequently been called SRG. However, mass migration and relief formation is not limited to formation of gratings, namely, irradiation though a patterned photomask or a single beam also induces migration as will be discussed below. Typical amorphous Az-containing polymers used for the mass transport studies and liquid-crystalline ones used in our investigations are indicated in Fig. 23 on the left and right hand side, respectively.

**4.1 Binary Component Systems.** Unique photo-activated mass migration systems were first proposed by Ubukata et al. using LC binary component materials comprised of 6Az10-PVA and 5CB.[141–143] This work was initiated as a serendipitous extension during evaluations of the command surface model using 6Az10-PVA/5CB hybrid LB films.[144–146] The hybrid films were irradiated with non-polarized UV (365 nm) light in advance to attain a cis-rich photo-equilibrated state (UV light treatment). Starting from this state, an argon ion laser (488 nm), which induced isomerization to the trans form, was used to induce film migration. The growth of the first-order diffraction efficiency monitored with a He-Ne laser and from morphological evaluation by using AFM indicates that mass migration is attained at very small dose levels ($<100\,\mathrm{mJ\,cm^{-2}}$), which is comparable to typical photoresist systems. The topographical AFM images in Fig. 22 indicate that even a short irradiation for 0.5 s at $10\,\mathrm{mW\,cm^{-2}}$ already

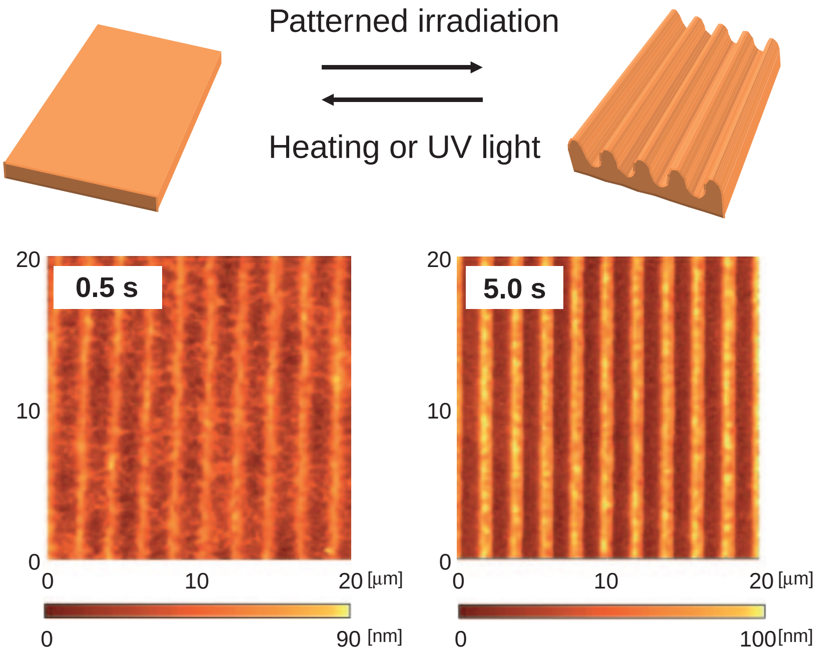

Fig. 22. Scheme of photo-induced or photo-triggered migration by holographic or patterned irradiation (upper), and typical examples of resulting SRG structure (lower) [Reproduced with modifications from *Adv. Mater.* **2000**, *12*, 1675, Copyright permission: Wiley] (Fig. 2).

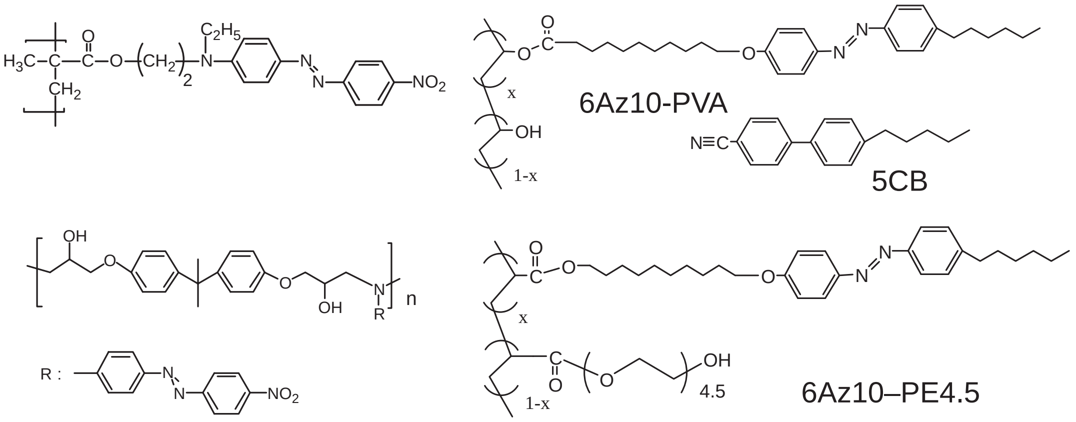

Fig. 23. Chemical structure of representative amorphous (left) and LC polymers (right) that are used for photo-induced or photo-triggered mass transport.

brings about SRG formation and that 5 s is sufficient to complete the mass migration. Here, the energy level is three orders of magnitude smaller than those required for conventional amorphous polymer systems hitherto reported. This means that the process, which formerly required several ten of minutes of illumination, can be shortened to levels with a beam of identical intensity.

Many types of calamitic (rod-like shaped) LCs as shown in Table 1 are incorporated in the 6Az10-PVA film. Some LC materials promote mass migration, and the others do not. Probably, a critical factor affecting this is the thermophysical state of the materials at room temperature (ca. 23–25 °C), i.e., whether the LC material adopts the nematic state or another higher ordered state at room temperature, at which experiments are made. Efficient photo-triggered mass transport occurs when the incorporated LC material is in the nematic state. The completely different behavior between 5CB and 5OCB should be noted. In terms of chemical structure, the two molecules are very similar. However, the former is in the nematic state, and the latter in the crystalline state at room temperature.

Figure 24 indicates an essential feature of this binary system. This figure shows the diffraction efficiency (closed circles) and the surface modulation depth (open circles, $\Delta h$) of the hybrid films at various molar fractions of 5CB ($f$) performed after UV light treatment. The diffraction efficiency suddenly increased at $f = 0.67$, which corresponds to the stoichiometry of two 5CB molecules per one Az unit. Below and above this ratio the diffraction efficiency rapidly decreased. The profile of $\Delta h$ almost follows that of the diffraction efficiency to give a maximum depth (100 nm) at $f = 0.67$. Differential scanning calorimetric analysis for the bulk mixtures[142] and the Langmuir monolayer experiments on water both show

Table 1. Behavior of Phototriggered Mass Transport of 6Az10-PVA Mixed with Various Calamitic Liquid Crystals

| Liquid crystal | Chemical structure | Phase transition temperature/°C[a)] | $\eta$/% | $\Delta h$/nm |
|---|---|---|---|---|
| 5CB | 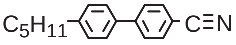 | K 23 N 35 I | 0.67 | 50–60 |
| DON-103 | 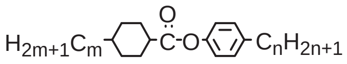 | K 14 N 73 I | 0.92 | 50–60 |
| NPC-02 | 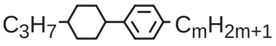 | K 16 N 35 I | 0.91 | 80–90 |
| MBBA | 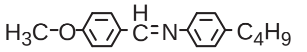 | K 22 N 47 I | 0.43 | 40–50 |
| RDP60774 | 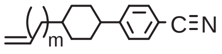 | K 13 N 43 I | 1.67 | 90–100 |
| RDP60716 | 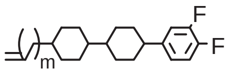 | K 8 N 115 I | 1.90 | 100–110 |
| 5OCB | 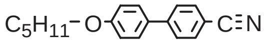 | K 48 N 67 I | 0.01 | — |
| 6OCB | 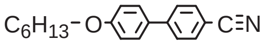 | K 56 N 76 I | 0.01 | — |
| 8OCB | 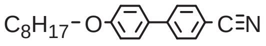 | K 55 A 67 N 80 I | 0.07 | — |
| TBBA |  | K 113 G 144 C<br>172 A 198 N 234 I | 0.02 | — |
| Pel-Chol | 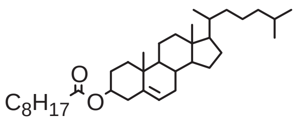 | K 81 Ch 92 I | 0.05 | — |

a) K: crystal, N: nematic, C: smectic C, A: smectic A, Ch: Cholesteric, I: isotropic, G: glass.

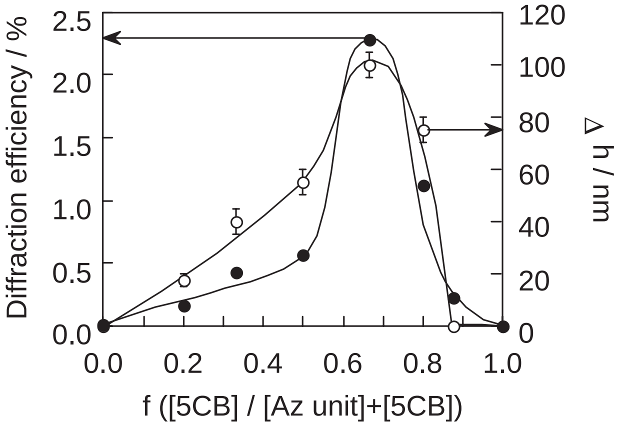

Fig. 24. Efficiency of photo-triggered mass transport vs. mol fraction of 5CB [Reproduced with modifications from *Adv. Mater.* **2000**, *12*, 1675, Copyright permission: Wiley] (Fig. 3).

that one 6Az10-side chain can accommodate two 5CB molecules. Therefore, 5CB acts not as only a plasticizer but provides the stoichiometric supramolecular material. The instant mass migration is the result from the cooperative interplay between 6Az10-PVA and 5CB.

**4.2 Oligo(ethylene oxide)-Containing Polymers.** Another important requirement for the relief forming materials is the shape stability in terms of long-term storage, and durability against water, organic vapors and heating. In this respect, the binary systems incorporating low-molecular-mass molecules have some drawbacks, because small molecules may evaporate at higher temperatures and long term usage. The stability can be improved when one employs amorphous polymers with high $T_g$[147,148] or liquid-crystalline polymers having high $T_i$ (transition temperature to isotropic state).[149] However, high $T_g$ or $T_i$ materials severely reduce the mass mobility.

Zettsu et al. have developed oligo(ethylene oxide) (EO)-containing liquid-crystalline polymers.[150–153] The polymer is synthesized by the random radical copolymerization of an EO-containing acrylate or methacrylate and Az-containing ones (6Az10-PE4.5, Fig. 23). Introduction of the EO chain causes effects similar to the incorporation of low-molecular-mass LC molecules, and efficient mass migration also occurs.

The single component copolymer, of course, possesses high stability and can be used repeatedly. Figure 25 displays the repeatability of this material. The left figure indicates changes in the intensity of first-order diffraction light caused by holographic irradiation and successive erasure by irradiation with UV light. The erasure of the SRG is due to a flattening caused by the surface tension of a fluidized film in the cis-rich state. As shown, the SRG writing and erasure could be repeated many times. The right figure is the optical microscopic image of surface relief structure irradiated through photomasks. The relief indicated as "11th writing" was obtained at the same position of the film of "First writing." No trace of memory (crosstalk) occurred after rewriting. In this way, complete era-

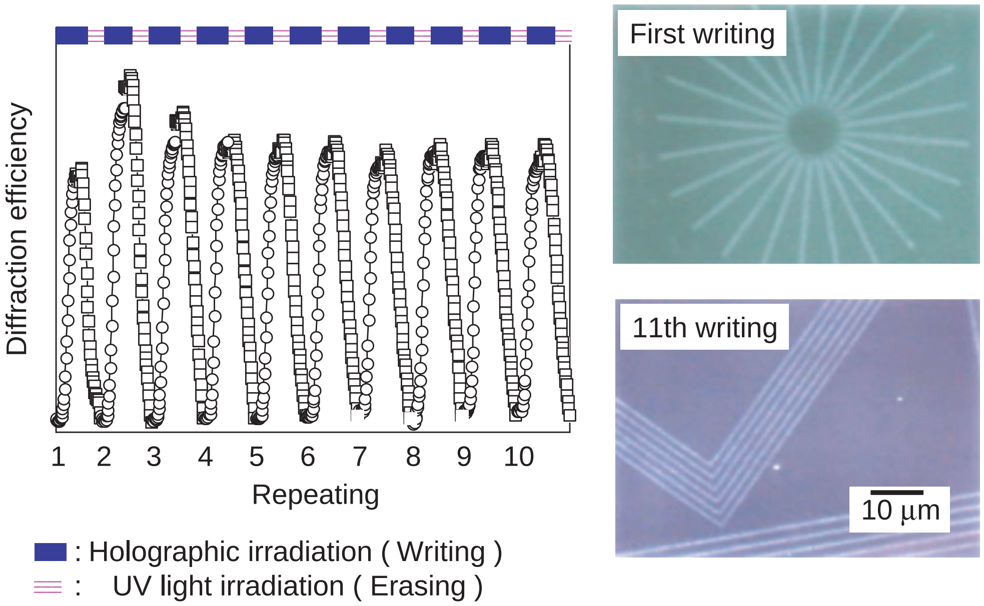

Fig. 25. Patterned photoalignment of mesochannels using a photomask. Photomask (upper) and the obtained silica film (lower) [Reproduced with modifications from *Macromolecules* **2004**, *37*, 8692, Copyright permission: American Chemical Society] (Fig. 5).

sure and resetting can be attained in this mass-transfer system. Reconstruction of the relief structures is a particular feature that cannot be realized in conventional photoresist systems, in which the polymer nature is chemically altered by photoirradiation.

**4.3 Fixation of the Relief Structure.** After the surface relief structure was formed, the polymer was then subjected to the chemical crosslinking via formalization (acetal formation with formaldehyde) between the hydroxy groups at the terminus in the EO chain. AFM observations justify the remarkable stability improvement after the crosslinking (Fig. 26). The SRG structure in the untreated film disappeared upon heating at 80 °C, whereas the surface modulation pattern in the formalized film remained even at 250 °C without any damage. The process employed here can be compared with a simple approach using Az polymers of high $T_g$. Fukuda et al.[147,148] have employed maleimide-based high $T_g$ amorphous polymer ($T_g = 170$–$279$ °C). In their polymer systems, the thermal stability is considerably improved; however, vast amounts of exposure energy was required. Light doses required for SRG inscription for such a high $T_g$ polymer typically range $>100\,\mathrm{J\,cm^{-2}}$. The soft and crosslinked 6Az10-PE4.5 is a unique strategy, in which mass migration is achieved in a soft state and immobilization can occur at any desired stage, providing marked thermal stability as compared to high $T_g$ polymers.

Once the crosslink is formed in the SRG film, the photoisomerization to the cis form does not alter the film morphology. This behavior is in marked contrast to the film before crosslinking, in which UV irradiation erases the SRG structure. Reversible photoisomerization occurred with retention of the SRG structure (Fig. 27). When low-molecular-mass LC was placed on the fixed film, the LC cell reversibly aligned changes between the homeotropic and homogeneous states upon alternate visible/UV light irradiation (Fig. 27, lower images).[152] In the homogeneous state, the LC molecules aligned parallel to the undulations of SRG. Here, the in-plane direction was controlled without irradiation with LPL. The surface geometry of the film governs the LC alignment.

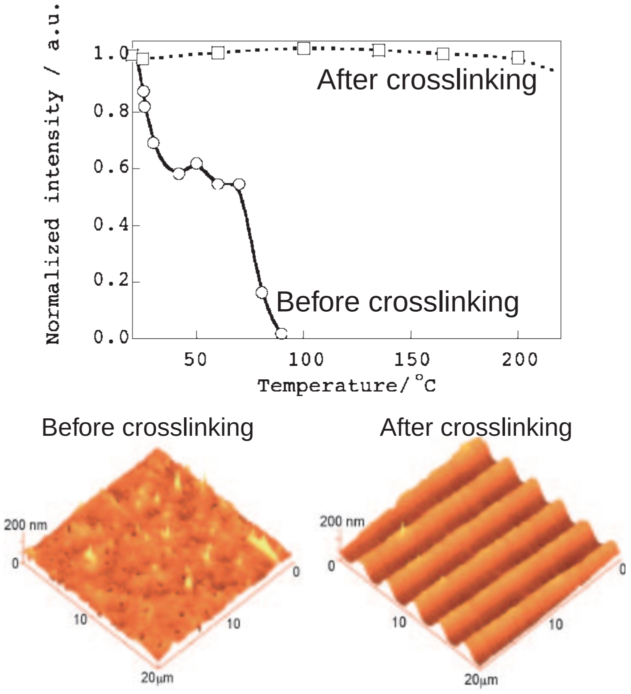

Fig. 26. Thermal stability of SRG structure of untreated and treated films with. Evaluation of temperature dependency (upper) and AFM images after heating 250 °C for 2 h [Reproduced with modifications from *Macromolecules* **2004**, *37*, 8692, Copyright permission: American Chemical Society] (Fig. 6).

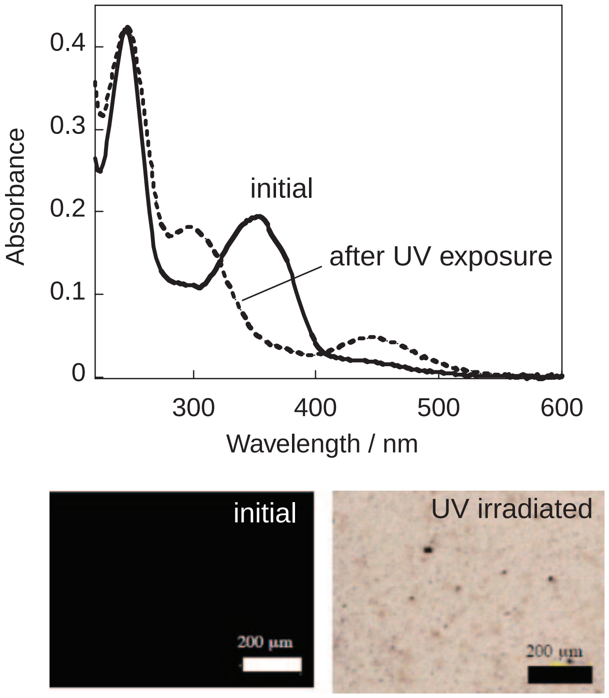

Fig. 27. UV–visible spectra after crosslinking (upper) and LC alignment behavior as command surface on the crosslinked SRG surface. LC is aligned in parallel with the SRG structure on UV irradiation [Reproduced with modifications from *Macromolecules* **2004**, *37*, 8692, Copyright permission: American Chemical Society] (Fig. 8).

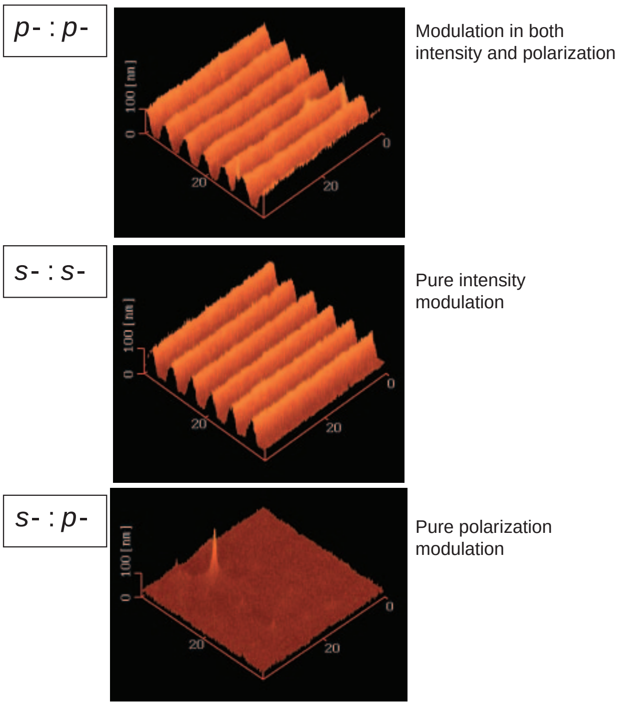

Fig. 28. SRG formation by double beam interference in different polarization modes.

**4.4 On the Mechanism of Mass Migration.** The mass migrating systems mentioned here have no polarization dependence, which shows marked contrast with widely known properties for hitherto investigated polymers. In general, the migration has a strong polarization dependency, and the migration proceeds in the direction of electric field of light.[138–140] The absence of polarization dependency in the instant mass migration systems can be explained by using two kinds of experiments; a double beam exposure experiment varying the polarizations configurations and irradiation through a patterned photomask with non-polarized light.

Figure 28 shows the topographical AFM images of SGR starting from the cis-rich Az polymer film under irradiation with different polarization combinations. Irradiation experiments were carried out under three types of polarization configurations. The (*p*-:*p*-), (*s*-:*s*-), and (*s*-:*p*-) modes provide intensity and polarization, pure intensity, and pure polarization holographic modulations, respectively. Under the intensity grating conditions (intensity holography), i.e., (*s*-:*s*-) and (*p*-:*p*-), the SRG readily formed. There was essentially no dependence of the SRG inscription rate under the two intensity holographic conditions.[154] On the other hand, when the two interfering beams were orthogonally polarized (*s*-:*p*-), (polarization holography), no growth of the diffraction intensity profile is observed. These behaviors are essentially different from other systems so far reported.

The lack of polarization dependence and migration in the dark clearly indicate that the processes involved in this effective mass migration are thermal in essence. The thermal driving factors can involve an attractive force that may work between the isotropic and LC phase, surface tension, dewetting etc. Also, mass transfer in the hybrid film continued even in the dark after switching off the light irradiation.[155,156] Such a spontaneous thermal process is related to dewetting observed in thin fluid polymer films. A recent study revealed that mass transfer occurs via indirect sensitization reaction from a near infrared absorbing dye.[153] In these contexts, the present process should be considered as "photo-triggered" thermally driven migration rather than a "photo-induced" one that expresses the photon-driven events.

**4.5 Conveyer Actions.** Thus far, applications of photoinduced migrations considered have been almost limited to utilization of the resulting static relief structures. They involve holographic recording, phase mask, LC alignment, waveguide couplers, fabrication of intricate surfaces, etc.[5,138,140] In the instant mass migrating system, the motion itself can be a valuable function. In this section, application as a "molecular conveyer" for patterning of light-inert (non-photoresponsive) functional materials is presented.[155] Functional materials, such as dye molecules, conjugated polymers, and semiconductor quantum dots, can be conveyed by the massive motion of the Az polymers (Fig. 29).

A blue rod-like diaminoanthraquinone-type dye was embedded into the hybrid film of 6Az10-PVA and 5CB. At higher dye content, e.g. 10 mol % of the LC molecule, UV irradiation, followed by dark adaptation at room temperature for a day, led to a growth of dendritic crystals of the dye. When crystallization was performed after photoinscription of the lined relief (18 µm width in this case), the direction of dye organization is restrained and aligned along the relief structure. After sufficient crystallization at room temperature, the protruding line

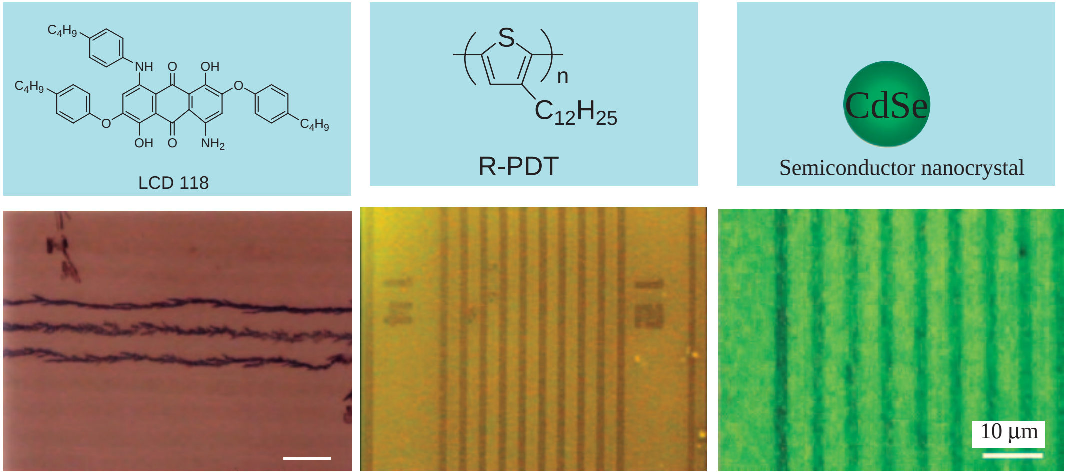

Fig. 29. Phototactic transport of functional materials (dye, p-conjugated polymer and nanocrystal) by conveyance actions [Reproduced with modifications from *Adv. Mater.* **2004**, *16*, 220, Copyright permission: Wiley] (Fig. 3).

showed high optical anisotropy. The polarized optical-microscope image indicated that the dichroic dye aligns in the direction of the inscribed line. The absorption moment of the dichroic dye was highly aligned parallel to the direction of the inscribed line. Most probably, the orientational anisotropy is induced by a uniaxial growth in the diffusion-limited crystallization restricted in the one-dimensional geometry.[155]

Application of the mass conveying principle is not limited to low-molecular-mass molecules; a larger material, e.g., semiconductor nanocrystals (NCs)[157] with a diameter of 6 nm molecular weight of $6 \times 10^5$ can be also conveyed.[155] Spin-cast films were prepared from a mixed solution composed of 6Az10-PVA, 5CB, and cadmium selenide (CdSe) NCs. After short light exposure through a grating photomask, surface relief undulations clearly formed. Observation of luminescence from NCs by fluorescence microscopy shows that NCs are transported following the patterned irradiation.

The conveying action may be widely applicable to many other kinds of functional materials that are themselves inert to light. A great advantage to using the instant migration system is that only small amounts of light, which would not damage the host materials, are required.

**4.6 Incorporation of Hierarchical Structures in the Relief Structure.** So far photo-induced or photo-triggered mass maigrations have been achieved for single-phase materials including homopolymers and random copolymers. Morikawa et al.[158] have introduced controlled hierarchical structures into the relief structure using a block copolymer ($p(EO_{114}–Az_{67})$) developed by Iyoda et al.[74] In the procedure adopted here, no laborious or costly lithographic substrate procedures are required. The key for the out-of-plane alignment (whether the cylinders orients normal or parallel to the substrate surface) is the film thickness and that for the in-plane control is direction of the linear polarization upon illumination.

After appropriate annealing and successive cooling down to room temperature, this copolymer film forms hexagonally packed PEO cylinders orienting normal to the substrate plane over long distance ranges in thin film due to its liquid crystallinity.[74] In flat films, the orientation of nanocylinder of PEO has clear thickness dependence. In the range of 30–60 nm thickness, the nanocylinders had a parallel (laid) orientation, and when the films became thicker than 70 nm, they adopted normal orientation with respect to the substrate surface. Iyoda et al.[159] have also reported the same observations on the thickness dependence. Thickness change of a polymer film can alter the nanostructures and their orientations for block copolymer systems[160] and also influence the orientation of mesogens with respect to the substrate.[161] The orientational change of the nanocylinders seems to be closely related to such phenomena.

Then, the two types of holographic irradiation ((*p*-:*p*-) and (*s*-:*s*-)) were performed. For the diblock copolymer under investigation, essentially no relief formation occurred (a) in the same procedure. When 5CB was mixed with $p(EO_{114}–Az_{67})$ (1:1 molar ratio with respect to Az unit), efficient mass migration occurred at a comparable high efficiency as for the case for the random copolymer (b).[141] The film was then subjected to the post-treatment. During the annealing procedure, 5CB molecules almost fully evaporated as confirmed by UV–visible spectroscopy.

Figure 30 shows the AFM images of the surface relief structure of the films after annealing where the thickness at the troughs is about 30 nm after annealing. Here, only the results obtained by (*p*-:*p*-) mode irradiation are shown. The phase mode image indicates that the cylinders were oriented perpendicular to the substrate plane at the areas of trough (b) and crest (d), respectively. Interestingly, the cylinder orientations changed critically with no graduations at the boundary area between the trough and crest (c). The parallel oriented (laid) cylinders at troughs aligned uniformly along the edges of the crests, i.e., perpendicular to the electric field vector of polarized light of holographic recording. The diameter of the core of PEO cylinder was 13 ± 1 nm in both areas. The average nearest-neighbor distance between the dots observed at the crest and that between the stripes at the trough were 23 ± 1 and 28 ± 2 nm, respectively. It is noteworthy that, when the trough of a relief-inscribed film is thicker them 70 nm, all of the cylinders adopt normal orientation regardless of the modulation shape. Therefore, the initial thickness is of essence for out-of-plane orientation discrimination.

The same holographic irradiation was made for the (*s*-:*s*-)

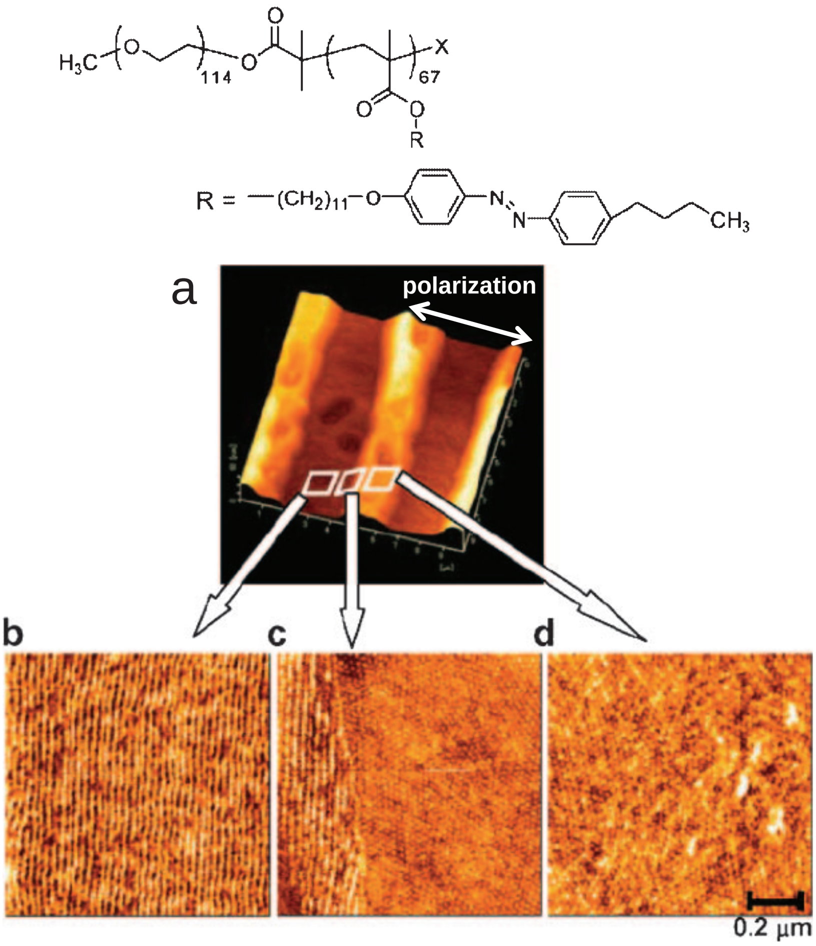

Fig. 30. Hierarchical structures involved in photo-generated SRG of a block copolymer. Topographical image (a), phase images at a trough (b), boundary (c), and crest (d) regions. [Reproduced with modifications from *Adv. Mater.* **2006**, *18*, 883, Copyright permission: Wiley] (Fig. 2).

mode configuration. The only difference is the direction of in-plane alignment of laid cylinders at the trough areas. Thus, the direction of the photo-oriented Az chromophore given caused by the linear polarization of the laser beam obviously governs the orientations of PEO cylinders in the trough parts. Thus, by combining thickness modulation and polarized light irradiation, both out-of-plane and in-plane controls are performed. The relationship between the polarization modes of holographic irradiation and the resulting hierarchical structure is shown in Fig. 31. It is stressed here that holographic irradiation leads to three different hierarchy levels, namely, molecular orientation (nm level), microphase-separated structure (several ten nm), and SRG (µm).

## 5. New Smart Photoresponsive Systems

**5.1 Photoinduced 3D Ordering and Patterning of Nanostructures.** Many efforts have been made to induce of macroscopic alignment of the microphase-separated structures. For example, application of an external field[162,163] and alignment via confinement of chemically or topologically surface-patterned substrates[164–167] have been performed. Approaches with light have started quite recently. The former section introduced the photochemical alignment of nanocylinders by holographic irradiation with LPL.[158] Yu et al.[168] have also shown macro-

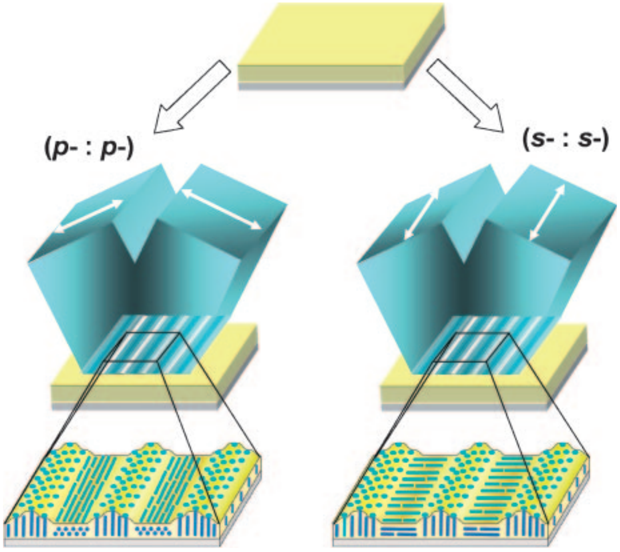

Fig. 31. Hierarchical structures of SRG of the block copolymer generated in different polarization modes [Reproduced with modifications from *Adv. Mater.* **2006**, *18*, 883, Copyright permission: Wiley] (Fig. 3).

scopic photoalignment of a closely related PEO based block copolymer for a flat film. The nanocylinders of PEO aligned orthogonal to the direction of the electric field vector of irradiated polarized light.

In view of thermal and mechanical stability, polystyrene (PS)-based block copolymers possessing higher $T_g$ are interesting.[169–172] This section introduces the first example of photoalignment and re-alignment of the microphase-separated structure in a PS-based block copolymer film produced by Morikawa et al.[173] The diblock copolymer used in this study is denoted as p($S_{76}$–$Az_{140}$) (Fig. 32). For macroscopic alignment by LPL, the following procedures were applied. LPL exposure (436 nm) was performed at 2.0 mW cm$^{-2}$ for 50 min at 130 °C (above the order–disorder transition), followed by gradual cooling to 30 °C at a rate of 2 °C min$^{-1}$. For evolution of the microphase-separated structure, the films were successively annealed at 107 °C, slightly above $T_g$ of PS block and below the $Sm_A$ transition to isotropic transition of the Az polymer block, for 12 h.

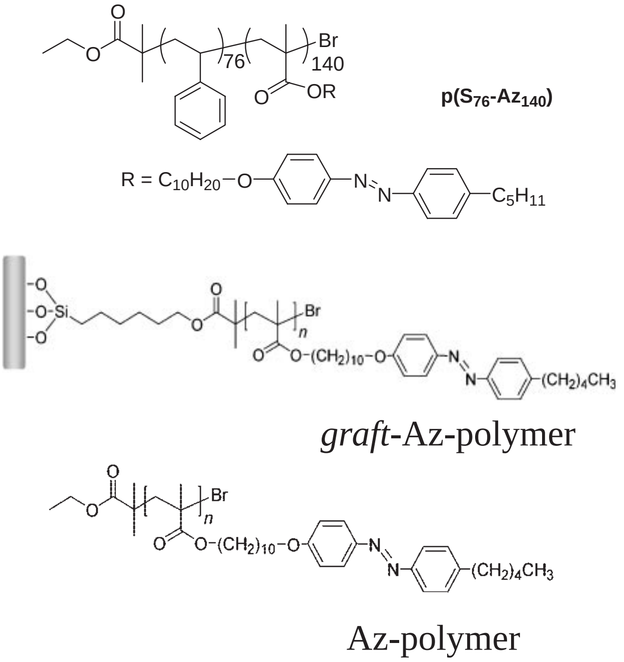

Fig. 32. Chemical structure and architecture of Az-containing polymers.

Figure 33 shows the nanocylinder alignment and re-alignment procedures. Non-irradiated films afforded PS cylinders in the upright orientation (a) after annealing. The diameter of the cylinders was 14 ± 1 nm with an average cylinder to cylinder distance of 32 nm. After LPL irradiation, a stripe morphology, of which the direction was highly controlled orthogonal to the direction of LPL, was observed (b). The Az group had a strong in-plane anisotropy with an orientational order parameter ($S$) of 0.68. A similar procedure was successively performed by using LPL set orthogonal to the previous irradiation angel (c). Essentially the same results from the MPS morphology and spectral data were obtained, except for the direction of the molecular orientation and morphology. The order parameter in the re-aligned state was also high ($S = 0.68$). The cylinders aligned in the in-plane direction reverted back to the out-of-plane (normal) mode upon irradiation with non-polarized light in the normal direction (d). The final state is the same as the initial state (a). These facts unequivocally indicate that 3D ordering, namely both in-plane and out-of-plane orientational control, of nanocylinder of PS domain can be achieved by using light.

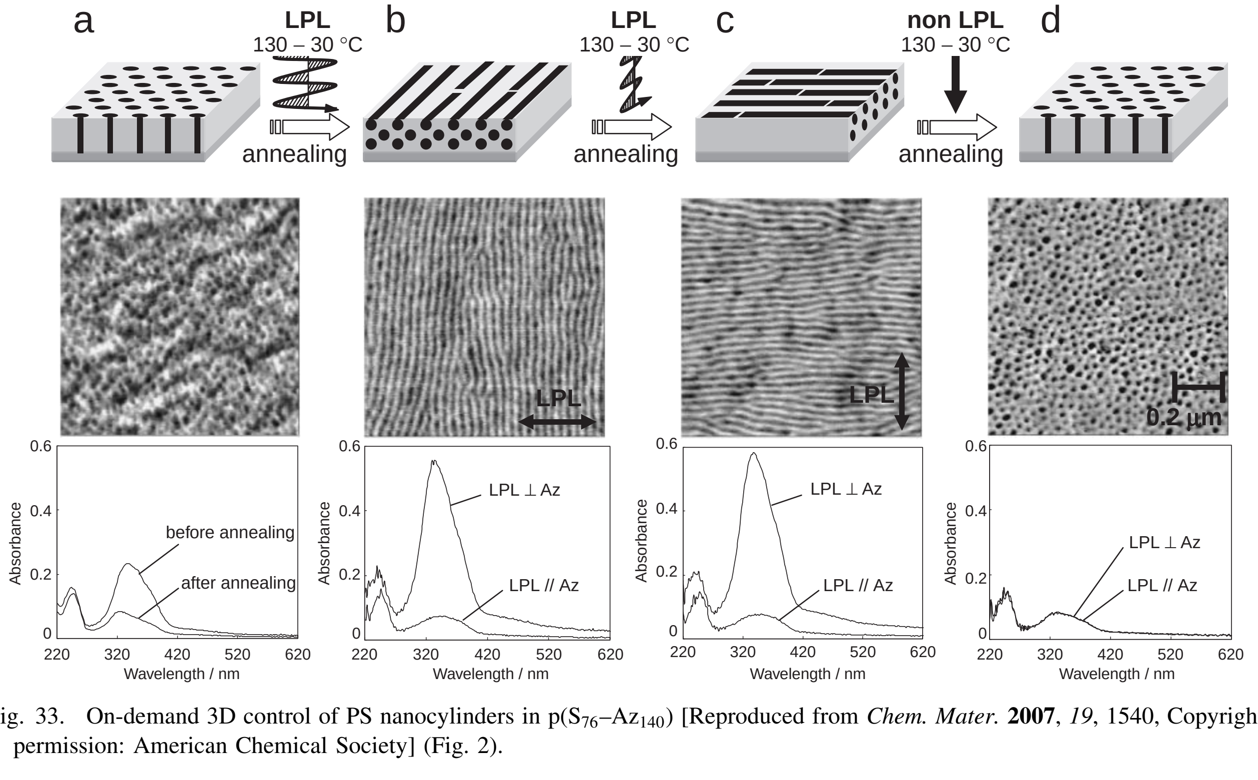

Fig. 33. On-demand 3D control of PS nanocylinders in p($S_{76}$–$Az_{140}$) [Reproduced from *Chem. Mater.* **2007**, *19*, 1540, Copyright permission: American Chemical Society] (Fig. 2).

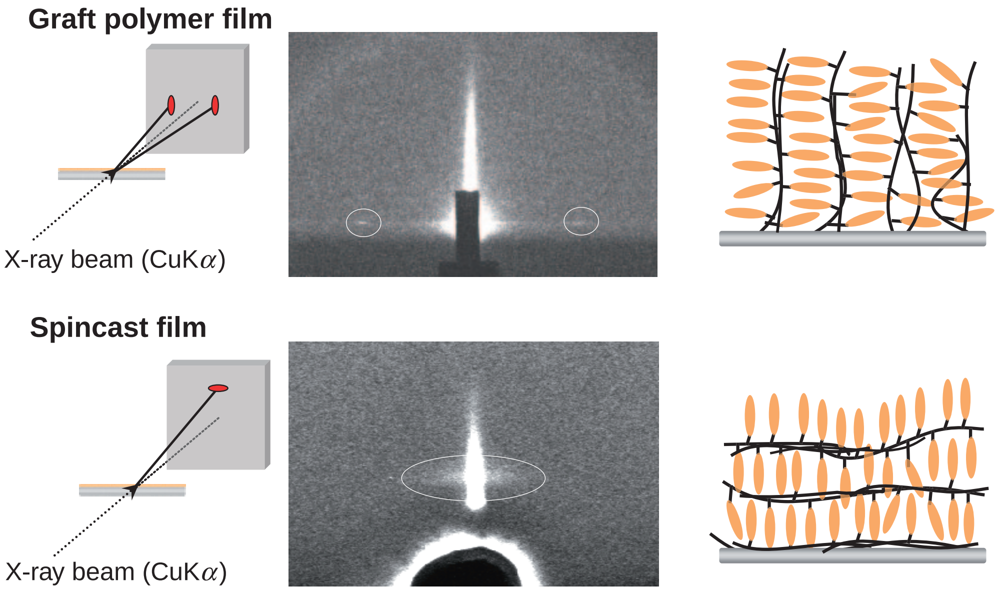

Fig. 34. Mesogenic and smectic layer orientation of grafted and spincast thin films of LC Az polymer [Reproduced with modifications from *Langmuir* **2007**, *23*, 4642, Copyright permission: American Chemical Society] (Figs. 2 and 4).

**5.2 Az-Containing Liquid Crystalline Grafted Polymer Films.** In recent years, polymer brushes have become fascinating subjects in polymer research. They are defined as dense layers of end-grafted polymer chains confined to a solid surface or interface.[174,175] Recently, high graft density and well-defined polymer brush structures have been developed using living radical polymerization, such as ATRP.[176–180] Since ATRP can be performed using various types of monomers, many functional polymer brushes can be designed.

Introduction of LC properties into the surface-graft chains seems of great interest in view of fabrication of “smart” responsive surfaces.[181–185] Uekusa et al.[186] have synthesized LC polymer brushes bearing an Az mesogenic group in side chains by adopting surface-initiated ATRP (*graft*-Az-polymer in Fig. 32). The polymer brushes have characteristic properties quite different and unpredictable from those of the spincast films. A unique orientation behavior of a smectic LC state in the thin films prepared by the surface-initiated polymerization is indicated. UV–visible spectroscopic measurements reveal that the Az mesogens adopt a parallel orientation in the film, which is in sharp contrast to that in spincast films of the same polymer (Az-polymer in Fig. 32). A normal orientation of the mesogenic groups is commonly observed for the spincast films of smectic LC Az polymer.[187,188]

The 2D XRD profile of the grafted polymer film recorded on an imaging plate is depicted in Fig. 34. Diffraction patterns are only observed in the in-plane direction, i.e., the periodic structures derived from the smectic LC phase are perpendicular to the substrate plane with LC mesogens being aligned parallel to the substrate. This orientation was observed for a first time for the homopolymer system only by tethering one terminal to the substrate. The figure also shows an 1D XRD pattern monitored in the in-plane direction. A clear peak was observed at $2\theta = 2.48°$, which corresponds to a layer spacing of 3.56 nm. This spacing corresponds to a long-range ordering of approximately the length of the fully extended Az side chain suggesting the formation of interdigitated structures of Az side chains. In contrast, a diffraction pattern on the spincast film of the homopolymer was observed only in the out-of-plane direction at $2\theta = 2.73°$ ($d = 3.26$ nm), which is derived from the smectic LC phase.

An in-plane orientation of mesogens is often observed in a microphase-separated state of LC block copolymers;[189,190] however, to our knowledge, this type of smectic LC orientation in a polymer film was observed for the first time. In the grafted LC polymer film, thermophysical properties were similar to those of a spincast film. The particular in-plane orientation of Az groups in the grafted polymer film may lead to different photo-responsive nature in the film. Since the photoresponsive mesogens are oriented parallel to the substrate plane, the film may be more sensitive to the polarization of LPL, and we are currently investigating this.

## 6. Concluding Remarks

It seems that attempts for creation of new functionalities using photoresponsive polymers are expanding rapidly. This is probably due to strong interest in molecular assemblies. In this regards, how we can transfer or amplify this molecular motion to larger hierarchies in the materials becomes a very important question. Design of flexible molecular assemblies with sufficient motional freedom becomes important. Approaches focusing onto monolayers and ultrathin polymer films introduced in this article seems very effective and reasonable. This article gave an overview of 1) large photomechanical effects in monolayers which can be extended to the study of photochemical modulations of 2D nanostructures formed by block copolymers, 2) orientational transfer of photooriented monolayers to LC, polymer materials, and mesostructured organic/inorganic nanomaterials, 3) light-driven efficient massive motions of organized Az-containing polymers including block copolymers, and finally 4) our recent approach to fabricate new smart responsive systems including block copolymer thin films and LC grafted polymers. The significance of polymer organization and handling at interfaces is not limited to interests in fabrication of light-responsive systems. We anticipate that similar strategies will yield various kinds of stimulus or environment-responsive functions of soft materials.

This article reported a few of the topics and the activities regarding monolayers or thin films thinner than 100 nm. For thicker films with thicknesses over micrometer, intensive studies are being undertaken for production of photonic materials and devices that can be used for holographic memories and light modulators.[6,10,191] New developments in organized Az-containing polymer and LC systems in Japan are worth describing. With regard to wetting properties, demonstration of light-driven liquid droplet by Ichimura et al.[192] and critical alternations in superhydrophilic and superhydrophobic surfaces based on the Az photoisomerization by Kim et al.[193] are worth mentioning. For photomechanical actuation, Ikeda et al. have developed new LC LC elastomer films[11] that show photoinduced bent or roll in response to light along the direction of rubbing[194] or LPL electric vector.[195] As light modulation systems, the structural color of a hydrogel obtained after templating of crystalline spheres[196,197] can be switched by the photoisomerization of an embedded Az unit reported by Takeoka et al.[198] Research on light modulation and memory/rewriting effects in cholesteric LC systems is also making marked progresses as shown by Tamaoki and Ajay Mallia[199] and Moriyama, Kato, et al.[200] A very recent work by Kobatake, Irie, et al.[201] indicates that even a photochromic crystal exhibits reversible bending and stretching upon irradiation, which can "bat" a small silica ball. In other words, the above-mentioned results together with light-driven thin film systems described here strongly show the versatility and utility of photoresponsive polymers as future materials.

The author thanks Prof. K. Ichimura for his long collaboration and encouragement. The author is much indebted to many co-workers and students in the Tokyo Institute of Technology (1995–2002) and Nagoya University (2003–present) for their great contributions and efforts. Special thanks are due to Dr. S. Nagano and Prof. Y. Takeoka of Nagoya University, and Drs. Ubukata, K. Fukuda, N. Zettsu, Y. Kawashima, T. Kobayashi, S. Kadota, H. Fukumoto, T. Uekusa, and Y. Morikawa for their key contributions to the work. Collaboration and encouraging discussions with Profs. K. Ito (Univ. Tokyo), T. Ikeda (Tokyo Tech.), T. Iyoda (Tokyo Tech.) and M. Nakagawa (Tokyo Tech.), and Drs. T. Tamaki (AIST), S. Morino (Hakusan Corp.), K. Arimitsu (Tokyo Univ. Sci.), N. Tamaoki (AIST), N. Mizoshita (Toyota Central Lab.) are greatly appreciated. The author also thanks Profs. N. Kawatsuki (Hyogo Univ.), H. Yamaoka (Univ. Shiga Pref.) and H. Matsuoka (Kyoto Univ.) and Dr. T. Fukuda (AIST) for valuable collaborations. The work has been financially supported by Grant-in-Aid for Scientific Research on Priority Areas (Nos. 277, 404, and 417) and Basic Research A (No. 16205019), Special Coordination Funds for Promoting Science and Technology from MEXT and JSPS, CREST program of the agency of Japan Science and Technology, Nissan Science Foundation, Shimadzu Science Foundation, and Asahi Glass Science Foundation.

## References

1 G. S. Hartley, *Nature* **1937**, *140*, 281.

2 G. S. Hartley, *J. Chem. Soc.* **1938**, 633.

3 L. M. Minsk, U.S. Patent 2725377, **1955**.

4 P. G. Egerton, E. Pitts, A. Reiser, *Macromolecules* **1981**, *14*, 95.

5 A. Natansohn, P. Rochon, *Chem. Rev.* **2002**, *102*, 4139.

6 *Photoreactive Organic Thin Films*, ed. by Z. Sekkat, W. Knoll, Academic Press, San Diego, CA, **2002**.

7 G. S. Kumar, D. C. Neckers, *Chem. Rev.* **1989**, *89*, 1915.

8 K. Ichimura, *Chem. Rev.* **2000**, *100*, 1847.

9 T. Seki, *Polym. J.* **2004**, *36*, 435.

10 T. Ikeda, *J. Mater. Chem.* **2003**, *13*, 2037.

11 T. Ikeda, J. Mamiya, Y. Yu, *Angew. Chem., Int. Ed.* **2007**, *46*, 506.

12 H. Rau, in *Photochemistry and Photophysics*, ed. by J. F. Rebeck, CRC Press, Boca Raton, **1990**, Chap. 4, p. 119.

13 H. Rau, *Photoisomerization of Azobenzenes*, in *Photoreactive Organic Thin Films*, ed. by Z. Sekkat, W. Knoll, Academic Press, San Diego, CA, **2002**, Chap. 1.

14 T. Seki, K. Ichimura, *Polym. Commun.* **1989**, *30*, 108.

15 T. Seki, K. Ichimura, *Thin Solid Films* **1989**, *179*, 77.

16 K. Nishiyama, M. Kurihara, M. Fujihira, *Thin Solid Films* **1989**, *179*, 477.

17 T. Seki, K. Ichimura, *Dynamic Photocontroled of Molecular Organization and Motion of Materials by Two-Dimensionally Arranged Azobenzene Assemblies*, in *Photoreactive Organic Thin Films*, ed. by Z. Sekkat, W. Knoll, Academic Press, San Diego, CA, **2002**, Chap. 15.

18 M. Irie, *Adv. Polym. Sci.* **1990**, *94*, 27.

19 H. S. Blair, H. I. Pague, J. E. Riordan, *Polymer* **1980**, *21*, 1195.

20 H. S. Blair, C. B. McArdle, *Polymer* **1984**, *25*, 1347.

21 B. R. Malcolm, O. Pieroni, *Biopolymers* **1990**, *29*, 1121.

22 B. R. Malcolm, *Thin Solid Films* **1989**, *178*, 17.

23 A. Ahluwalia, R. Piolanti, D. De Rossi, *Langmuir* **1997**, *13*, 5909.

24 O. N. Oliveira, Jr., D. M. Taylor, H. Morgan, *Thin Solid Films* **1992**, *210–211*, 76.

25 H. Menzel, *Macromol. Chem. Phys.* **1994**, *195*, 3747.

26 H. Menzel, M. L. Hallensleben, *Polym. Bull.* **1991**, *27*, 89.

27 H. Menzel, *Macromolecules* **1993**, *26*, 6226.

28 C. Steinem, A. Janshoff, M. S. Vollmer, M. R. Ghadiri, *Langmuir* **1999**, *15*, 3956.

29 M. S. Vollmer, T. D. Clark, C. Steinem, M. R. Ghadiri, *Angew. Chem., Int. Ed.* **1999**, *38*, 1598.

30 J. W. Weener, E. W. Meijer, *Adv. Mater.* **2000**, *12*, 741.

31 A. Sidorenko, C. Houphouet-Boigny, O. Villavicencio, M. Hashemzadeh, D. V. McGrath, V. V. Tsukruk, *Langmuir* **2000**, *16*, 10569.

32 T. Seki, T. Tamaki, *Chem. Lett.* **1993**, 1739.

33 T. Seki, R. Fukuda, M. Yokoi, T. Tamaki, K. Ichimura, *Bull. Chem. Soc. Jpn.* **1996**, *69*, 2375.

34 T. Seki, H. Sekizawa, R. Fukuda, T. Tamaki, M. Yokoi, K. Ichimura, *Polym. J.* **1996**, *28*, 613.

35 K. Kago, M. Fuerst, H. Matsuoka, H. Yamaoka, T. Seki, *Langmuir* **1999**, *15*, 2237.

36 J. C. MacDonald, G. M. Whitesides, *Chem. Rev.* **1994**, *94*, 2383.

37 T. Kato, *Science* **2002**, *295*, 2414.

38 T. Seki, T. Fukuchi, K. Ichimura, *Bull. Chem. Soc. Jpn.* **1998**, *71*, 2807.

39 T. Seki, T. Fukuchi, K. Ichimura, *Langmuir* **2000**, *16*, 3564.

40 T. Seki, T. Fukuchi, K. Ichimura, *Langmuir* **2002**, *18*, 5462.

41 T. Kobayashi, T. Seki, K. Ichimura, *Chem. Commun.* **2000**, 1193.

42 T. Kobayashi, T. Seki, *Langmuir* **2003**, *19*, 9297.

43 J. Glazer, A. E. Alexander, *Trans. Faraday Soc.* **1951**, *47*, 401.

44 T. Kato, H. Akiyama, M. Yoshida, *Chem. Lett.* **1992**, 565.

45 Y. Urai, C. Ohe, K. Itoh, M. Yoshida, K. Iimura, T. Kato, *Langmuir* **2000**, *16*, 3920.

46 Q. Huo, S. Russev, T. Hasegawa, J. Nishijo, J. Umemura, G. Puccetti, K. C. Russell, R. M. Leblanc, *J. Am. Chem. Soc.* **2000**, *122*, 7890.

47 T. Kobayashi, T. Seki, *Kobunshi Ronbunshu* **2003**, *60*, 569.

48 D. Hönig, D. Möbius, *J. Phys. Chem.* **1991**, *95*, 4590.

49 S. Hénon, J. Meunier, *Rev. Sci. Instrum.* **1991**, *62*, 936.

50 T. Seki, H. Sekizawa, K. Ichimura, *Polymer* **1997**, *38*, 725.

51 T. Seki, H. Sekizawa, S. Morino, K. Ichimura, *J. Phys. Chem. B* **1998**, *102*, 5313.

52 T. Seki, H. Sekizawa, K. Ichimura, *Polym. J.* **1999**, *31*, 1079.

53 T. Seki, K. Tanaka, K. Ichimura, *Macromolecules* **1997**, *30*, 6401.

54 T. Seki, J. Kojima, K. Ichimura, *Macromolecules* **2000**, *33*, 2709.

55 D. Beaglehole, E. Z. Radlinska, B. W. Ninham, H. K. Christenson, *Phys. Rev. Lett.* **1991**, *66*, 2084.

56 Y. L. Chen, J. N. Israelachivili, *J. Phys. Chem.* **1992**, *96*, 7752.

57 M. Matsumoto, D. Miyazaki, M. Tanaka, R. Azumi, E. Manda, Y. Kondo, N. Yoshino, H. Tachibana, *J. Am. Chem. Soc.* **1998**, *120*, 1479.

58 M. Matsumoto, S. Terrettaz, H. Tachibana, *Adv. Colloid Interface Sci.* **2000**, *87*, 147.

59 T. Seki, J. Kojima, K. Ichimura, *J. Phys. Chem. B* **1999**, *103*, 10338.

60 K. Blodgett, *Phys. Rev.* **1937**, *51*, 964.

61 M. K. Kurnaz, D. K. Schwartz, *Langmuir* **1996**, *12*, 4971.

62 P. F. Green, R. Limary, *Adv. Colloid Interface Sci.* **2001**, *94*, 53.

63 G. Kraush, *Mater. Sci. Eng.* **1995**, *14*, 1.

64 K. Liu, S. M. Baker, M. Tuominen, T. P. Russell, I. K. Schuller, *Phys. Rev. B* **2001**, *63*, 060403.

65 M. Park, C. Harrison, P. M. Chaikin, R. A. Register, D. H. Adamson, *Science* **1997**, *276*, 1401.

66 C. Park, J. Yoon, E. L. Thomas, *Polymer* **2003**, *44*, 6725.

67 G. Widawski, M. Rawiso, B. François, *Nature* **1994**, *369*, 387.

68 A. Sidorenko, I. Tokaref, S. Minko, M. Stamm, *J. Am. Chem. Soc.* **2003**, *125*, 12211.

69 T. Thurn-Albrecht, J. Schotter, G. A. Kästle, N. Emley, T. Shibauchi, L. Krusin-Elbaum, K. Guarini, C. T. Black, M. T. Tuominen, T. P. Russell, *Science* **2000**, *290*, 2126.

70 J. K. Cox, K. Yu, B. Constantine, A. Eisenberg, B. Lennox, *Langmuir* **1999**, *15*, 7714.

71 J. Zhu, B. Lennox, A. Eisenberg, *J. Phys. Chem.* **1992**, *96*, 4727.

72 J. Kumaki, T. Hashimoto, *J. Am. Chem. Soc.* **2003**, *125*, 4907.

73 S. Kadota, K. Aoki, S. Nagano, T. Seki, *J. Am. Chem. Soc.* **2005**, *127*, 8266.

74 Y. Tian, K. Watanabe, X. Kong, J. Abe, T. Iyoda, *Macromolecules* **2002**, *35*, 3739.

75 Y. Frere, F. Yang, P. Gramain, D. Guillon, A. Skoulios, *Makromol. Chem.* **1988**, *189*, 419.

76 S. Kadota, K. Aoki, S. Nagano, T. Seki, *Colloids Surf., A* **2006**, *284–285*, 535.

77 N. Sato, S. Ito, M. Yamamoto, *Macromolecules* **1998**, *31*, 2673.

78 J. Kumaki, T. Hashimoto, *J. Am. Chem. Soc.* **1998**, *120*, 423.

79 J. Zhu, A. Eisemberg, R. B. Lennox, *J. Am. Chem. Soc.* **1991**, *113*, 5583.

80 M.-V. Meli, A. Badia, P. Grütter, R. B. Lennox, *Nano Lett.* **2002**, *2*, 131.

81 S. M. Baker, K. A. Leach, C. E. Devereaux, D. E. Gragson, *Macromolecules* **2000**, *33*, 5432.

82 C. E. Devereaux, S. M. Baker, *Macromolecules* **2002**, *35*, 1921.

83 Q. Lu, C. G. Bazuin, *Nano Lett.* **2005**, *5*, 1309.

84 D. J. Crisp, *J. Colloid Sci.* **1946**, *1*, 161.

85 J. Kumaki, *Macromolecules* **1986**, *19*, 2258.

86 T. Kajiyama, Y. Oishi, *Trends Polym. Sci.* **1995**, *3*, 30.

87 G. L. Gaines, Jr., *Langmuir* **1991**, *7*, 834.

88 S. Nagano, T. Seki, K. Ichimura, *Langmuir* **2001**, *17*, 2199.

89 S. Nagano, T. Seki, *J. Am. Chem. Soc.* **2002**, *124*, 2074.

90 S. Nagano, Y. Matsushita, Y. Ohnuma, S. Shinma, T. Seki, *Langmuir* **2006**, *22*, 5233.

91 K. Ichimura, Y. Suzuki, T. Seki, A. Hosoki, K. Aoki, *Langmuir* **1988**, *4*, 1214.

92 T. Seki, M. Sakuragi, Y. Kawanishi, T. Tamaki, R. Fukuda, K. Ichimura, Y. Suzuki, *Langmuir* **1993**, *9*, 211.

93 M. O'Neill, S. K. Kelly, *J. Phys. D: Appl. Phys.* **2000**, *33*, R67.

94 T. Seki, K. Fukuda, K. Ichimura, *Langmuir* **1999**, *15*, 5098.

95 K. Fukuda, T. Seki, K. Ichimura, *Macromolecules* **2002**, *35*, 2177.

96 K. Fukuda, T. Seki, K. Ichimura, *Macromolecules* **2002**, *35*, 1951.

97 R. D. Miller, J. Michl, *Chem. Rev.* **1989**, *89*, 1359.

98 R. H. Tredgold, R. A. Allen, P. Hodge, E. Khoshdel, *J. Phys. D: Appl. Phys.* **1987**, *20*, 1385.

99 A. Natansohn, P. Rochon, M. Pozolét, P. Audet, D. Brown, S. To, *Macromolecules* **1994**, *27*, 2580.

100 S. R. Andrews, G. Williams, L. Lasker, J. Stumpe, *Macromolecules* **1995**, *28*, 8463.

101 Th. Geue, A. Ziegler, J. Stumpe, *Macromolecules* **1997**, *30*, 5729.

102 C. Ruslim, K. Ichimura, *Adv. Mater.* **2001**, *13*, 37.

103 K. Ichimura, S. Furumi, S. Morino, M. Kidowaki, M. Nakagawa, M. Ogawa, Y. Nishiura, *Adv. Mater.* **2000**, *12*, 950.

104 K. Ichimura, M. Momose, T. Fujiwara, *Chem. Lett.* **2000**, 1022.

105 M. Kidowaki, T. Fujiwara, K. Ichimura, *Chem. Lett.* **1999**, 643.

106 C. W. Frank, V. Rao, M. M. Despotopoulou, R. F. W. Pease, W. D. Hinsberg, R. D. Miller, J. F. Rabolt, *Science* **1996**, *273*, 912.

107 C. T. Kresge, M. E. Leonowicz, W. J. Roth, J. C. Varatuli, J. S. Beck, *Nature* **1992**, *359*, 710.

108 T. Yanagisawa, T. Shimizu, K. Kuroda, C. Kato, *Bull. Chem. Soc. Jpn.* **1990**, *63*, 988.

109 H. Miyata, K. Kuroda, *Chem. Mater.* **1999**, *11*, 1609.

110 H. Miyata, K. Kuroda, *Adv. Mater.* **1999**, *11*, 1448.

111 Y. Kawashima, M. Nakagawa, T. Seki, K. Ichimura, *Chem. Mater.* **2002**, *14*, 2842.

112 Y. Kawashima, M. Nakagawa, K. Ichimura, T. Seki, *J. Mater. Chem.* **2004**, *14*, 328.

113 H. Fukumoto, S. Nagano, N. Kawatsuki, T. Seki, *Adv. Mater.* **2005**, *17*, 1035.

114 H. Fukumoto, S. Nagano, N. Kawatsuki, T. Seki, *Colloids Surf., A* **2006**, *284–285*, 309.

115 H. Fukumoto, S. Nagano, N. Kawatsuki, T. Seki, *Chem. Mater.* **2006**, *18*, 1226.

116 N. Kawatsuki, T. Kawakami, T. Yamamoto, *Adv. Mater.* **2001**, *13*, 1337.

117 N. Kawatsuki, K. Goto, T. Kawakami, T. Yamamoto, *Macromolecules* **2002**, *35*, 706.

118 M. Schadt, H. Seiberle, A. Schuster, *Nature* **1996**, *381*, 212.

119 M. Schadt, K. Schmitt, V. Kozinkov, V. Chingrinov, *Jpn. J. Appl. Phys.* **1992**, *31*, 2155.

120 M. Obi, S. Morino, K. Ichimura, *Jpn. J. Appl. Phys.* **1999**, *38*, L145.

121 A. Hozumi, Y. Yokogawa, T. Kameyama, K. Hiraku, H. Sugimura, O. Takai, M. Okido, *Adv. Mater.* **2000**, *12*, 985.

122 H. Fukumoto, S. Nagano, T. Seki, *Chem. Lett.* **2006**, *35*, 180.

123 H. Hasebe, K. Takeuchi, H. Takatsu, *J. Photopolym. Sci. Technol.* **1997**, *10*, 25.

124 H. Takatsu, H. Hasebe, *Ekisho* **1999**, *3*, 34.

125 A. Hozumi, Y. Yokogawa, T. Kameyama, K. Hikaru, H. Sugimura, O. Takai, M. Okido, *Adv. Mater.* **2000**, *12*, 985.

126 M. Eich, J. H. Wendorff, B. Reck, H. Ringsdorf, *Makromol. Chem., Rapid Commun.* **1987**, *8*, 59.

127 S. Ivanov, I. Yakovlev, S. Kostromin, V. Shibaev, L. Läsker, J. Stumpe, D. Kreysig, *Makromol. Chem., Rapid Commun.* **1991**, *12*, 709.

128 J. Stumpe, L. Müller, D. Kreysig, G. Hauck, H. D. Koswig, R. Ruhmann, J. Rübner *Makromol. Chem., Rapid Commun.* **1991**, *12*, 81.

129 A. Natansohn, P. Rochon, J. Gosselin, S. Xie, *Macromolecules* **1992**, *25*, 2268.

130 T. Ikeda, O. Tsutsumi, *Science* **1995**, *268*, 1873.

131 P. Rochon, E. Batalla, A. Natansohn, *Appl. Phys. Lett.* **1995**, *66*, 136.

132 D. Y. Kim, S. K. Tripathy, L. Li, J. Kumar, *Appl. Phys. Lett.* **1995**, *66*, 1166.

133 P. S. Ramanujam, N. C. R. Holme, S. Hvilsted, *Appl. Phys. Lett.* **1996**, *68*, 1329.

134 J. Kumar, L. Li, X. L. Jiang, D. Y. Kim, T. S. Lee, S. K. Tripathy, *Appl. Phys. Lett.* **1998**, *72*, 2096.

135 C. J. Barrett, P. Rochon, A. Natansohn, *J. Chem. Phys.* **1998**, *109*, 1505.

136 P. S. Ramanujam, M. Pedersen, S. Hvilsted, *Appl. Phys. Lett.* **1999**, *74*, 3227.

137 K. Sumaru, T. Yamanaka, T. Fukuda, H. Matsuda, *Appl. Phys. Lett.* **1999**, *75*, 1878.

138 N. K. Viswanathan, D. Y. Kim, S. Bian, J. Williams, W. Liu, L. Li, L. Samuelson, J. Kumar, S. K. Tripathy, *J. Mater. Chem.* **1999**, *9*, 1941.

139 K. G. Yager, C. J. Barrett, *Curr. Opin. Solid State Mater. Sci.* **2001**, *5*, 487.

140 O. N. Oliveira, Jr., J. Kumar, L. Li, S. K. Tripathy, *Surface-Relief Gratings on Azobenzene-Containing Films*, in *Photoreactive Organic Thin Films*, ed. by Z. Sekkat, W. Knoll, Academic Press, San Diego, CA, **2002**, Chap. 14, p. 429.

141 T. Ubukata, T. Seki, K. Ichimura, *Adv. Mater.* **2000**, *12*, 1675.

142 T. Ubukata, T. Seki, K. Ichimura, *Colloids Surf., A* **2002**, *198*, 113.

143 T. Ubukata, M. Hara, T. Seki, *Mol. Cryst. Liq. Cryst.* **2002**, *377*, 173.

144 T. Ubukata, T. Seki, K. Ichimura, *J. Phys. Chem. B* **2000**, *104*, 4141.

145 T. Ubukata, T. Seki, S. Morino, K. Ichimura, *J. Phys. Chem. B* **2000**, *104*, 4148.

146 T. Ubukata, T. Seki, K. Ichimura, *Polym. J.* **2001**, *33*, 891.

147 T. Fukuda, H. Matsuda, N. Viswanathan, S. K. Tripathy, J. Kumar, T. Shiraga, M. Kato, H. Nakanishi, *Synth. Met.* **1999**, *102*, 1435.

148 T. Fukuda, H. Matsuda, T. Shiraga, T. Kimura, M. Kato, N. Viswanathan, J. Kumar, S. K. Tripathy, *Macromolecules* **2000**, *33*, 4220.

149 L. Andruzzi, A. Altomare, F. Ciardelli, R. Solaro, S. Hvilsted, P. S. Ramanujam, *Macromolecules* **1999**, *32*, 448.

150 N. Zettsu, T. Ubukata, T. Seki, K. Ichimura, *Adv. Mater.* **2001**, *13*, 1693.

151 N. Zettsu, T. Fukuda, H. Matsuda, T. Seki, *Appl. Phys. Lett.* **2003**, *83*, 4960.

152 N. Zettsu, T. Seki, *Macromolecules* **2004**, *37*, 8692.

153 N. Zettsu, T. Ogasawara, R. Arakawa, S. Nagano, T. Ubukata, T. Seki, *Macromolecules* **2007**, *40*, 4607.

154 N. Zettsu, T. Fukuda, H. Matsuda, T. Seki, *Appl. Phys. Lett.* **2003**, *83*, 4960.

155 T. Ubukata, M. Hara, K. Ichimura, T. Seki, *Adv. Mater.* **2004**, *16*, 220.

156 T. Ubukata, T. Higuchi, N. Zettsu, T. Seki, M. Hara, *Colloids Surf., A* **2005**, *257–258*, 123.

157 C. B. Murray, D. J. Norris, M. G. Bawendi, *J. Am. Chem. Soc.* **1993**, *115*, 8706.

158 Y. Morikawa, S. Nagano, K. Watanabe, K. Kamata, T. Iyoda, T. Seki, *Adv. Mater.* **2006**, *18*, 883.

159 K. Watanabe, R. Watanabe, D. Aoki, S. Shoda, M. Komura, K. Kamata, T. Iyoda, *Trans. Mater. Res. Soc. Jpn.* **2006**, *31*, 327.

160 A. Knoll, A. Horvat, K. S. Lyakhova, G. Krausch, G. J. A. Sevink, A. V. Zvelindovsky, R. Magerle, *Phys. Rev. Lett.* **2002**, *89*, 035501-1.

161 H. Mensinger, M. Stamm, C. Boeffel, *J. Chem. Phys.* **1992**, *96*, 3183.

162 T. L. Morkved, M. A. Lu, M. Urbas, E. E. Ehrichs, H. M. Jaeger, P. Mansky, T. P. Russell, *Science* **1996**, *273*, 931.

163 T. T. Albrecht, J. Schotter, G. A. Kästle, N. Emley, T. Shibauchi, L. K. Elbaum, K. Guarini, C. T. Black, M. T. Touminen, T. P. Russell, *Science* **2000**, *290*, 2126.

164 S. O. Kim, H. H. Solak, M. P. Stoykovich, N. J. Ferrier, J. J. de Pablo, P. F. Nealey, *Nature* **2003**, *424*, 411.

165 M. P. Stoykovich, M. Müller, S. O. Kim, H. H. Solak, E. W. Edwards, J. J. de Pablo, P. F. Nealey, *Science* **2005**, *308*, 1442.

166 R. A. Segalman, H. Yokoyama, E. J. Kramer, *Adv. Mater.* **2001**, *13*, 1152.

167 D. Sundrani, S. B. Darling, S. J. Sibener, *Nano Lett.* **2004**, *4*, 273.

168 H.-F. Yu, T. Iyoda, T. Ikeda, *J. Am. Chem. Soc.* **2006**, *128*,

11010.
169 G. Mao, J. Wang, S. R. Clingman, C. K. Ober, J. T. Chen, E. L. Thomas, *Macromolecules* **1997**, *30*, 2556.
170 C. Frenz, A. Fuchs, H.-W. Schmidt, U. Theissen, D. Haarer, *Macromol. Chem. Phys.* **2004**, *205*, 1246.
171 M. Häckel, L. Kador, D. Kropp, C. F. Renz, H.-W. Schmidt, *Adv. Funct. Mater.* **2005**, *15*, 1722.
172 X. Tong, L. Cui, Y. Zhao, *Macromolecules* **2004**, *37*, 3101.
173 Y. Morikawa, T. Kondo, S. Nagano, T. Seki, *Chem. Mater.* **2007**, *19*, 1540.
174 *Polymer Brushes*, ed. by R. C. Advincula, W. J. Brittain, K. C. Caster, J. Rühe, WILEY-VCH, **2004**.
175 S. T. Milner, *Science* **1991**, *251*, 905.
176 Y. Tsujii, K. Ohno, S. Yamamoto, A. Goto, T. Fukuda, *Adv. Polym. Sci.* **2006**, *197*, 1.
177 S. Edmondson, V. L. Osborne, W. T. S. Huck, *Chem. Soc. Rev.* **2004**, *33*, 14.
178 M. Ejaz, S. Yamamoto, K. Ohno, Y. Tsujii, T. Fukuda, *Macromolecules* **1998**, *31*, 5934.
179 B. Zhao, W. J. Brittain, *J. Am. Chem. Soc.* **1999**, *121*, 3557.
180 K. Matyjaszewski, P. J. Miller, N. Shukla, B. Immaraporn, A. Gelman, B. B. Luokala, T. M. Siclovan, G. Kickelbick, T. Vallant, H. Hoffmann, T. Pakula, *Macromolecules* **1999**, *32*, 8716.
181 D. R. M. Williams, A. Halperin, *Macromolecules* **1993**, *26*, 4208.
182 A. Halperin, D. R. M. Williams, *J. Phys.: Condens. Matter* **1994**, *6*, A297.
183 A. Halperin, D. R. M. Williams, *Annu. Rev. Mater. Sci.* **1996**, *26*, 279.
184 B. Peng, D. Johannsmann, J. Rühe, *Macromolecules* **1999**, *32*, 6759.
185 P. J. Hamelinck, W. T. S. Huck, *J. Mater. Chem.* **2005**, *15*, 381.
186 T. Uekusa, S. Nagano, T. Seki, *Langmuir* **2007**, *23*, 4642.
187 T. Geue, A. Zieglar, J. Stumpe, *Macromolecules* **1997**, *30*, 5729.
188 M. Han, S. Morino, K. Ichimura, *Chem. Lett.* **1999**, 645.
189 H. Fischer, S. Poser, *Acta Polym.* **1996**, *15*, 949.
190 G. Mao, J. Wang, S. R. Clingman, C. K. Ober, J. T. Chen, E. L. Thomas, *Macromolecules* **1997**, *30*, 2556.
191 T. Ikeda, A. Kanazawa, *Bull. Chem. Soc. Jpn.* **2000**, *73*, 1715.
192 K. Ichimura, S.-G. Oh, M. Nakagawa, *Science* **1997**, *277*, 1232.
193 H.-S. Kim, J.-T. Han, D.-H, Kwak, K.-W. Cho, *J. Am. Chem. Soc.* **2006**, *128*, 14458.
194 T. Ikeda, M. Nakano, Y. Yu, O. Tsutsumi, A. Kanazawa, *Adv. Mater.* **2003**, *15*, 201.
195 Y. Yu, M. Nakano, T. Ikeda, *Nature* **2003**, *425*, 145.
196 Y. Takeoka, M. Watanabe, *Adv. Mater.* **2003**, *15*, 199.
197 Y. Takeoka, T. Seki, *Langmuir* **2006**, *22*, 10223.
198 K. Matsubara, M. Watanabe, Y. Takeoka, *Angew. Chem., Int. Ed.* **2007**, *46*, 1688.
199 V. Ajay Mallia, N. Tamaoki, *Chem. Soc. Rev.* **2004**, *33*, 76.
200 M. Moriyama, N. Mizoshita, T. Yokota, K. Kishimoto, T. Kato, *Adv. Mater.* **2003**, *15*, 1335.
201 S. Kobatake, S. Takami, H. Muto, T. Ishikawa, M. Irie, *Nature* **2007**, *446*, 778.

Takahiro Seki was born in Tokyo in 1957. He received Bachelor and Master degrees in Polymer Chemistry from Tokyo Institute of Technology in 1979 and 1982, respectively. He received his Ph.D. from Tokyo Institute of Technology in 1986 on stimuli responsive permeation control in artificial lipid bilayers. He started an academic career at Tokyo Institute of Technology as a research associate. During 1986–1995 he held positions at the institutes of Agency of Industrial Science and Technology (AIST) at Tsukuba, the Research Institute of Polymers and Textiles (1986–1992) and the National Institute of Chemical and Materials Research (1993–1995). Form 1995 to 2002, he was an Associated Professor in the Chemical Resources Laboratory of Tokyo Institute of Technology and promoted to Professor of the Graduate School of Engineering, Nagoya University in 2002. He received The SPSJ Wiley Award in 2002, The Japanese Liquid Crystal Society Outstanding Paper Award in 2005, and The Chemical Society of Japan Award for Creative Work for 2006. His current research interests include photochromic polymers, organized molecular and polymer films, and liquid-crystalline materials.